De Novo Mutations Affecting the Catalytic Cα Subunit of PP2A, *PPP2CA*, Cause Syndromic Intellectual Disability Resembling Other PP2A-Related Neurodevelopmental Disorders

Sara Reynhout,[1,2,29] Sandra Jansen,[3,29] Dorien Haesen,[1,2] Siska van Belle,[1,2] Sonja A. de Munnik,[3] Ernie M.H.F. Bongers,[4] Jolanda H. Schieving,[5] Carlo Marcelis,[4] Jeanne Amiel,[6,7] Marlène Rio,[7] Heather Mclaughlin,[8] Roger Ladda,[9] Susan Sell,[9] Marjolein Kriek,[10] Cacha M.P.C.D. Peeters-Scholte,[11] Paulien A. Terhal,[12] Koen L. van Gassen,[12] Nienke Verbeek,[12] Sonja Henry,[13] Jessica Scott Schwoerer,[13] Saleem Malik,[14] Nicole Revencu,[15] Carlos R. Ferreira,[16] Ellen Macnamara,[16,17] Hilde M.H. Braakman,[18] Elise Brimble,[19] Maura R.Z. Ruznikov,[19,20] Matias Wagner,[21,22,23] Philip Harrer,[23] Dagmar Wieczorek,[24,25] Alma Kuechler,[25] Barak Tziperman,[26] Ortal Barel,[27,28] Bert B.A. de Vries,[3] Christopher T. Gordon,[6] Veerle Janssens,[1,2,30,*] and Lisenka E.L.M. Vissers[3,30,*]

Type 2A protein phosphatases (PP2As) are highly expressed in the brain and regulate neuronal signaling by catalyzing phospho-Ser/Thr dephosphorylations in diverse substrates. PP2A holoenzymes comprise catalytic C-, scaffolding A-, and regulatory B-type subunits, which determine substrate specificity and physiological function. Interestingly, *de novo* mutations in genes encoding A- and B-type subunits have recently been implicated in intellectual disability (ID) and developmental delay (DD). We now report 16 individuals with mild to profound ID and DD and a *de novo* mutation in *PPP2CA*, encoding the catalytic Cα subunit. Other frequently observed features were severe language delay (71%), hypotonia (69%), epilepsy (63%), and brain abnormalities such as ventriculomegaly and a small corpus callosum (67%). Behavioral problems, including autism spectrum disorders, were reported in 47% of individuals, and three individuals had a congenital heart defect. *PPP2CA de novo* mutations included a partial gene deletion, a frameshift, three nonsense mutations, a single amino acid duplication, a recurrent mutation, and eight non-recurrent missense mutations. Functional studies showed complete PP2A dysfunction in four individuals with seemingly milder ID, hinting at haploinsufficiency. Ten other individuals showed mutation-specific biochemical distortions, including poor expression, altered binding to the A subunit and specific B-type subunits, and impaired phosphatase activity and C-terminal methylation. Four were suspected to have a dominant-negative mechanism, which correlated with severe ID. Two missense variants affecting the same residue largely behaved as wild-type in our functional assays. Overall, we found that pathogenic *PPP2CA* variants impair PP2A-B56(δ) functionality, suggesting that PP2A-related neurodevelopmental disorders constitute functionally converging ID syndromes.

Introduction

Neurodevelopmental disorders (NDDs) represent a collection of clinically heterogeneous disorders—including intellectual disability (ID), epilepsy, and various behavioral disorders—and can manifest as an isolated cognitive defect or in combination with other comorbidities, such as congenital abnormalities.[1,2] Until recently, identifying the genetic etiology of NDDs remained challenging because of their extensive clinical and genetic heterogeneity. Recent advances

[1]Laboratory of Protein Phosphorylation & Proteomics, Department of Cellular & Molecular Medicine, University of Leuven (KU Leuven), 3000 Leuven, Belgium; [2]Leuven Brain Institute, PO Box 901, 3000 Leuven, Belgium; [3]Department of Human Genetics, Donders Institute for Brain, Cognition, and Behaviour, Radboudumc, PO Box 9101, 6500 HB Nijmegen, the Netherlands; [4]Department of Human Genetics, Radboudumc, PO Box 9101, 6500 HB Nijmegen, the Netherlands; [5]Department of Neurology, Radboudumc, PO Box 9101, 6500 HB Nijmegen, the Netherlands; [6]Laboratory of Embryology and Genetics of Human Malformations, Paris Descartes University, Sorbonne Paris Cité University and INSERM U1163, Institut Imagine, 75015 Paris, France; [7]Service de Génétique, Hôpital Necker – Enfants Malades, Assistance Publique – Hôpitaux de Paris, 75015 Paris, France; [8]GeneDx, 207 Perry Parkway, Gaithersburg, MD 20877, USA; [9]Penn State Hershey Children's Hospital, Hershey, PA 17033, USA; [10]Department of Clinical Genetics, Leiden University Medical Center, PO Box 9600, 2300 RC Leiden, the Netherlands; [11]Department of Neurology, Leiden University Medical Center, PO Box 9600, 2300 RC Leiden, the Netherlands; [12]Department of Genetics, University Medical Center Utrecht, PO Box 85500, 3508 GA Utrecht, the Netherlands; [13]Biochemical Genetics Clinic, University of Wisconsin School of Medicine and Public Health, University of Wisconsin, Madison, WI 53705, USA; [14]Comprehensive Epilepsy Program, Jane and John Justin Neuroscience Center, Cook Children's Medical Center, Fort Worth, TX 76104, USA; [15]Centre de Génétique Humaine, Cliniques Universitaires Saint-Luc, Université Catholique de Louvain, Avenue Hippocrate 10–1200, Brussels, Belgium; [16]Office of the Clinical Director, National Human Genome Research Institute, National Institutes of Health, Bethesda, MD 20892, USA; [17]NIH Undiagnosed Diseases Program, Common Fund, National Human Genome Research Institute, National Institutes of Health, Bethesda, MD 20892, USA; [18]Department of Neurology, Academic Center for Epileptology, Kempenhaeghe & Maastricht UMC+, Sterkelseweg 65, 5591 VE Heeze, the Netherlands; [19]Department of Neurology and Neurological Sciences, Stanford University School of Medicine, Stanford, CA, 94305, USA; [20]Department of Pediatrics, Division of Medical Genetics, Stanford Medicine, Stanford, CA 94305, USA; [21]Institute of Human Genetics, Helmholtz Zentrum München, 85764 Munich, Germany; [22]Institute of Human Genetics, Klinikum rechts der Isar, Technische Universität München, 81675 Munich, Germany; [23]Institute of Neurogenomics, Helmholtz Zentrum München, 85764 Munich, Germany; [24]Institute of Human Genetics, Medical Faculty, Heinrich-Heine-University Düsseldorf, 40225 Düsseldorf, Germany; [25]Institut für Humangenetik, Universitätsklinikum Essen, Universität Duisburg-Essen, 45147 Essen, Germany; [26]Pediatric Neurology Unit, Sheba Medical Center, 52621 Ramat Gan, Israel; [27]Genomic Unit, Sheba Cancer Research Center, Sheba Medical Center, 52621 Tel Hashomer, Israel; [28]Wohl Institute for Translational Medicine, Sheba Medical Center, 52621 Tel Hashomer, Israel
[29]These authors contributed equally to this work
[30]These authors contributed equally to this work
*Correspondence: veerle.janssens@kuleuven.be (V.J.), lisenka.vissers@radboudumc.nl (L.E.L.M.V.)
https://doi.org/10.1016/j.ajhg.2018.12.002.

in whole-exome sequencing (WES) and whole-genome sequencing have highlighted *de novo* mutations as a major cause of ID,[2–9] resulting in an increase in new clinical NDD entities associated with ID and developmental delay (DD).[1]

Recently, recurrent *de novo* mutations in genes encoding specific subunits of type 2A protein phosphatases (PP2As) have been reported,[3,4,10–12] establishing this phosphatase family as a novel and important player in the etiology of ID and DD. PP2A enzymes catalyze dephosphorylation of phospho-Ser and phospho-Thr residues in a large variety of substrates, thereby counterbalancing Ser/Thr-specific protein kinases and thus playing essential regulatory roles in cellular signaling.[13] Structurally, PP2As are holoenzymes comprising three subunits: a catalytic C-type, a scaffolding A-type, and a regulatory B-type subunit, the latter of which is of major importance in determining physiological functions, substrate specificity, and regulation of the complex.[14–16] PP2A complexes are encoded by 19 different genes, and mutations in three of these genes—*PPP2R1A* (MIM: 605983; subunit Aα), *PPP2R5C* (MIM: 601645; subunit B56γ), and *PPP2R5D* (MIM: 601646; subunit B56δ)[3,4,10–12]—have been conclusively identified as causes of ID and DD syndromes; for two others—*PPP2R5B* (MIM: 601644; subunit B56β)[11] and *PPP2R2C* (MIM: 605997; subunit B55γ)—variants in individuals with ID and DD have been observed.[17]

So far, detailed studies on *de novo* mutations in both genes encoding the C subunit (*PPP2CA* and *PPP2CB*) have not been reported. Yet, ID- and DD-related mutations in genes involved in C subunit regulation, such as *IGBP1* (MIM: 300472),[18] *MID1* (MIM: 300552),[19] and *BOD1* (MIM: 616745),[20,21] have been identified. Together with mutations in other PP2A subunits, these observations make the genes encoding the C subunit themselves excellent candidates for ID and DD disorders. Here, we report that *de novo* mutations in *PPP2CA*, encoding the PP2A catalytic Cα subunit, cause an ID and DD syndrome phenotypically characterized by mild to severe ID and DD, behavioral problems, variable types of epilepsy, hypotonia, and structural brain abnormalities. In addition, we provide functional evidence for a mutation-specific pathophysiological mechanism resulting in at least a common impairment of PP2A-B56δ holoenzyme functionality. Our data further highlight the importance of PP2A function in neurodevelopment.

Material and Methods

Generation of *PPP2CA* Mutants

To study the functional consequences of *de novo* missense mutations, we cloned the coding region of wild-type (WT) Cα cDNA into an N-terminally HA-tagged eukaryotic expression vector (pMB001) by using XbaI and BamHI sites. Mutated Cα constructs were directly generated from this pMB001 vector through PCR-based site-directed mutagenesis (Stratagene) with proofreading Pwo polymerase (Roche Applied Science) and complementary DNA oligonucleotide primers (Sigma Genosys) containing the desired point mutations (primer sequences in Table S1). To generate the Cα p.Phe308dup variant, we directly incorporated the mutation into the reverse Cα stop primer. We cloned the coding region, PCR-amplified with a Cα start primer and this mutated stop primer (primer sequences in Table S1), into pMB001 by using XbaI and BamHI restriction sites. All mutations were confirmed by sequencing (LGC Genomics).

Cellular PP2A Binding Assays

HEK293T cells were transfected with PEI transfection reagent according to a standard protocol. 48 hr after transfection, cells were rinsed with PBS, lysed in 200 μL NET buffer (50 mM Tris HCl [pH 7.4], 150 mM NaCl, 15 mM EDTA, and 1% Nonidet P-40) containing protease and a phosphatase inhibitor cocktail (Roche Applied Science), and centrifuged for 15 min at 13,000 × *g*. If the experiment required measuring of phosphatase activity, TBS was used instead of PBS, and phosphatase inhibitors were omitted from the lysis buffer.

For pull-down experiments, cell lysates were incubated at 4°C for 1 hr with 500 μL NENT100 buffer (20 mM Tris HCl [pH 7.4], 1 mM EDTA, 0.1% Nonidet P-40, 25% glycerol, and 100 mM NaCl) containing 1 mg/mL bovine serum albumin (BSA) and 30 μL monoclonal anti-HA-Agarose antibody beads (Sigma-Aldrich; for HA pull-down), 30 μL glutathione-Sepharose beads (GE Healthcare; for GST pull-down), or 30 μL GFP-trap-A beads (ChromoTek; for GFP trapping) on a rotating wheel. The beads were washed twice with 0.5 mL NENT100 containing 1 mg/mL BSA and twice with 0.5 mL NENT300 containing 300 mM NaCl.

In all cases, bound proteins were eluted by the addition of 2× NuPage sample buffer (Invitrogen) and boiling. The eluted proteins were subsequently analyzed by SDS-PAGE on 4%–12% (w/v) Bis-Tris gels (Bio-Rad) and immunoblotting. The membranes were blocked in 5% milk solution in TBS and 0.1% Tween-20 for 1 hr at room temperature (RT) and subsequently incubated with the primary antibody overnight at 4°C. The following primary mouse antibodies were used: anti-HA (Sigma-Aldrich), anti-GST (Sigma-Aldrich), anti-GFP (generously supplied by Dr. P. Parker at the Francis Crick Institute, London, UK), anti-PP2A-A subunit (generously supplied by Dr. S. Dilworth at Middlesex University, London, UK), anti-demethyl-PP2A clone 1D7 (BioLegend), anti-FLAG M2 (Sigma-Aldrich), anti-vinculin (Sigma-Aldrich), and anti-alpha4 clone 5F6 (Millipore).

After being washed in TBS and 0.1% Tween-20, the membranes were incubated at RT for 1 hr with horseradish-peroxidase-conjugated secondary antibodies (Dako) and developed on an ImageQuant LAS 4000 system (GE Healthcare) with a WesternBright ECL detection kit (Advansta). All densitometric quantifications were done with ImageJ software.

HA Peptide Elution

For binding experiments with the HA-tagged p.Arg214* Cα mutant, anti-HA-agarose-bound proteins were eluted for 30 min at 4°C after the final washing step by the addition of HA peptide (Sigma-Aldrich) at 200 ng/μL. The remaining beads were spun down, and the eluate was transferred for further use.

PP2A Activity Assays

After HA pull-down, beads were washed once more with 20 mM Tris HCl (pH 7.4) and 1 mM DTT (Tris-DTT) and finally resuspended in 80 μL Tris-DTT solution. All assays were performed with 20 μL of this "phosphatase suspension" and 9 μL of 2 mM stock of K-R-pT-I-R-R phosphopeptide for 20–40 min at 30°C (still in the linear range of the assay). The released free phosphate was

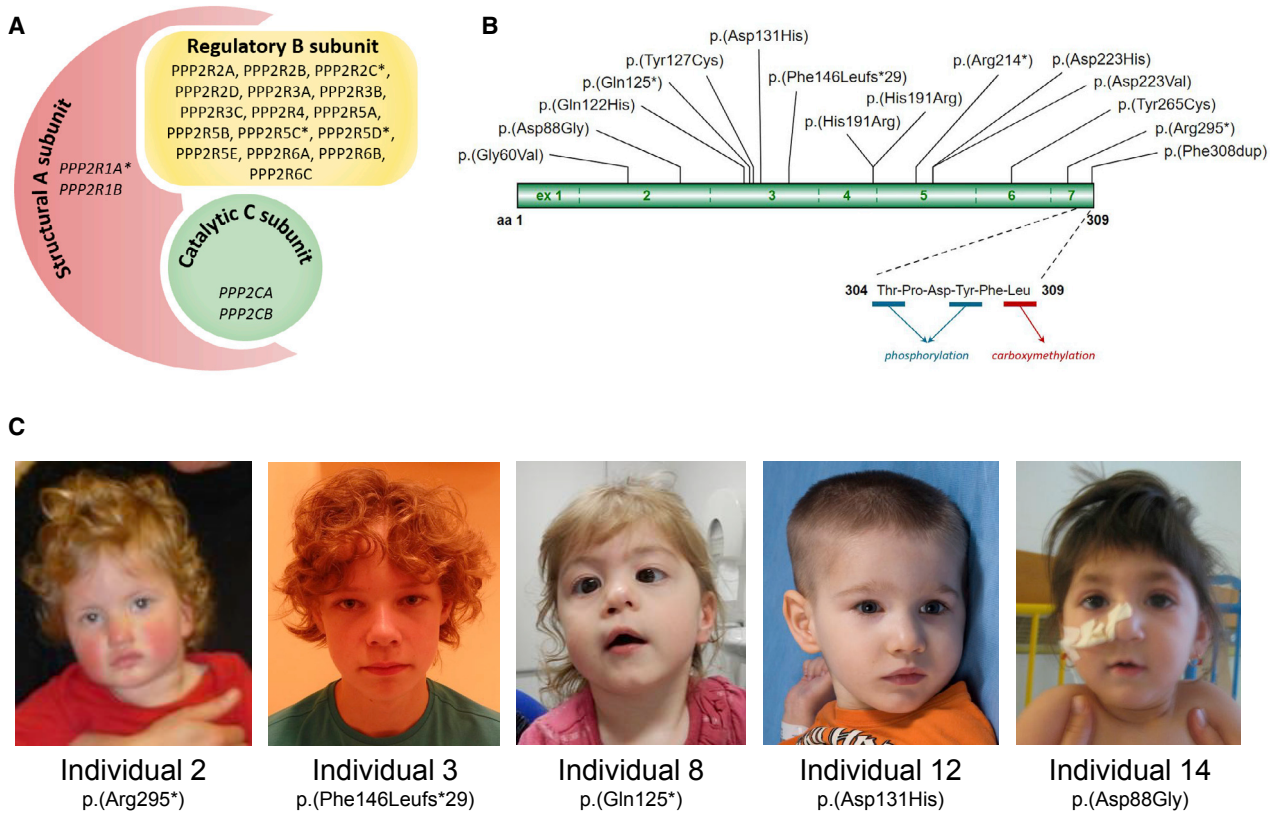

Figure 1. Schematic Overview of the PP2A Complex, Variants in the PP2A Catalytic Cα Subunit, and Photographs of Individuals
(A) Overview of the PP2A complex based on the canonical subunits. Gene names encoding the subunit components are listed in each subunit. *PPP2CA* encodes the catalytic subunit alpha, highlighted in green. Subunits known for their involvement in ID and DD are annotated with an asterisk.
(B) *De novo* mutations identified in individuals with ID and DD are shown with respect to their exonic and Cα protein localization; exon notation is indicated in the ribbon protein structure. The C-tail sequence involved in carboxymethylation and phosphorylation is enlarged for visualization purposes. Note that the partial deletion is not depicted.
(C) Facial features of individuals with a *de novo* mutation in *PPP2CA*. Some individuals had mild dysmorphisms, but a consistent facial gestalt was not observed. Informed consent was provided by the parents.

determined by the addition of BIOMOL Green (catalog no. BML-AK111-0250, Enzo). After 20 min of incubation at RT, absorbance at 620 nm was measured in a multi-channel spectrophotometer. We subsequently obtained specific phosphatase activity by correcting the measured absorbance for the input of HA-tagged Cα, as determined by immunoblotting with anti-HA antibodies and signal quantification by ImageJ.

Statistics

Statistical analysis of biochemical data was assessed with one-sample Student's t tests in which the data were compared with WT values that were set at 100% in each experimental replicate. p values below 0.05 were considered significant.

Results

Clinical Spectrum Associated with *PPP2CA* Mutations

Through international collaboration,[2,22] we recruited 16 individuals with a *de novo* mutation in *PPP2CA* (Figures 1A and 1B). This study was approved by the local institutes under the realm of diagnostic testing. Detailed clinical information is provided in the Supplemental Note and summarized in Table 1. Individuals were 1.5–23 years old and had mild to profound ID and DD, and ten had severe language impairment that was worse than expected in several individuals given their level of development. Behavioral problems, of which autism spectrum disorders (ASDs) were most frequently diagnosed, were noted in 7 of 15 individuals (47%). One individual (individual 7) also had psychotic episodes after which she had progressive cognitive dysfunction and worsening behavioral problems. Regression of development was also noted in individual 3. Ten individuals (63%) had seizures, albeit in different forms: two showed fever-related seizures, one was diagnosed with epileptic encephalopathy, two had focal seizures (one of whom was diagnosed with focal electrical status epilepticus during sleep), two had generalized tonic-clonic seizures, one was diagnosed with Jeavons syndrome, one had hypsarrhythmia, and one had an unknown type of seizures. Brain imaging was performed in 15 individuals and showed dilated ventricles (4/15), delayed myelination (2/15), and dysplasia or absence of the corpus callosum (4/15). Two individuals had macrocephaly, one of whom was also tall, and five individuals had

Table 1. Main Clinical Features of Individuals

General Information	Individual 1	Individual 2	Individual 3	Individual 4	Individual 5	Individual 6	Individual 7	Individual 8
Age	6 y	7 y	13 y	3 y, 10 m	19 y	2 y, 4 m	23 y	2 y, 1 m
Gender	male	female	male	male	female	female	female	Female
Chr change (hg19)	g.133536680T>C	g.133533511dup	g.133537587del	g.133533469_133533471dup	g.133536124G>A	g.133536680T>C	g.133536096T>A	g.133537652G>A
GenBank: NM_002715.2	c.572A>G	c.882dup	c.438del	c.922_924dup	c.640 C>T	c.572A>G	c.668A>T	c.373C>T
Protein change	p.His191Arg	p.Arg295*	p.Phe146Leufs*29	p.Phe308dup	p.Arg214*	p.His191Arg	p.Asp223Val	p.Gln125*
Mutation type	missense	nonsense	frameshift	1 amino acid insertion	nonsense	missense	missense	nonsense
Inheritance	*de novo*	*de novo*	*de novo*	*de novo*	*de novo*	*de novo*	*de novo*	*de novo*
Other variants?[a]	−	+	−	−	+	−	+	+
Proposed mechanism	haploinsufficiency of PP2A-B56δ complexes	dominant-negative effect on PP2A-B56δ complexes	haploinsufficiency: null allele (no expression)	dominant-negative effect on all PP2A-B56 complexes	haploinsufficiency: null allele (latent complex with alpha 4)	haploinsufficiency of PP2A-B56δ complexes	unclear	haploinsufficiency: null allele (no expression)
Growth								
Height	+2 SD	+2.5 SD	+1.3 SD	+1.7 SD	−0.2 SD	0 SD	+0.7 SD	−1.3 SD
Head circumference	+2.5 SD	+0.5 SD	−1.5 SD	−3.9 SD	NK	−0.2 SD	+2.8 SD	−0.8 SD
Weight	−0.2 SD	0 SD	−1.1 SD	+0.7 SD	>+2.5 SD	NK	NK	−0.6 SD
Neurological								
DD and ID (degree)	+ (mild)	+ (severe)	+ (mild)	+ (moderate)	+ (mild to moderate)	+ (mild)	+ (mild)	+ (mild)
Severe language delay	+	+	+	+	+	NK	−	−
Regression	−	−	+	−	−	−	+ (after period with psychoses)	−
Behavioral problems	−	+ (automutilation, stereotypic behavior)	+ (PDD-NOS)	−	+ (ASD, ADHD)	NK	+ (ASD, psychoses)	−
Hypotonia	−	+	+	−	+	−	+ (mild)	+
Epilepsy (type)	+ (related to fever)	+ (tonic-clonic seizures, absences)	+ (focal left temporal, mostly at night)	−	+ (generalized tonic-clonic seizures, absences)	+ (related to fever, tonic-clonic seizures)	−	−
Epilepsy syndrome	NA	epileptic encephalopathy	focal ESES	NA	Jeavons syndrome	NA	NA	NA
Age of onset	11 m	6 m	10 y	NA	6 y	NK	NA	NA
Age of offset	18 m	ongoing	ongoing	NA	ongoing	NK	NA	NA
Brain abnormalities	+ (ventriculomegaly)	+ (ventriculomegaly, gracile corpus callosum, delayed myelinization)	−	+ (posterior hypoplasia of corpus callosum, unmyelinated left temporal lobe, nonspecific periventricular white-matter hyperintensities)	−	+ (mildly underdeveloped pons, mesencephalon, mild dilated lateral and third ventricles)	−	+ (reduced white matter [supratentorial and infratentorial], some global atrophy of the brain [pons and corpus callosum], bilateral plexus choroideus cysts)
Other	−	sleeping difficulties	−	−	burning pain from neck down to left leg	−	−	broad-based gait

(*Continued on next page*)

Individual 9	Individual 10	Individual 11	Individual 12	Individual 13	Individual 14	Individual 15	Individual 16	Total (Percentage)
1 y, 9 m	8 y	2 y, 4 m	11 y	12 m	4 y	3 y, 4 m	7 y	NA
male	female	male	male	male	female	male	male	9 males, 7 females
g.133537645T>C	g.133534840T>C	deletion at chr5: 133, 546,961–133,667,321	g.133537634C>G	g.133537659C>G	g.133541662T>C	g.133541746C>A	g.133536097C>G	NA
c.380A>G	c.794A>G	NA	c.391G>C	c.366G>C	c.263A>G	c.179G>T	c.667G>C	NA
p.Tyr127Cys	p.Tyr265Cys	NA	p.Asp131His	p.Gln122His	p.Asp88Gly	p.Gly60Val	p.Asp223His	NA
missense	missense	partial deletion	missense	missense	missense	missense	missense	NA
de novo	*de novo*	*de novo*	*de novo*	*de novo*	*de novo*	*de novo*	*de novo*	NA
−	−	+	−	+	−	−	−	NA
haploinsufficiency of PP2A-B56 and PR72 complexes; dominant-negative effect on PP2A-B55 and PP2A-STRN complexes	haploinsufficiency: significant impairment of any trimer formation	haploinsufficiency (deletion)	haploinsufficiency of PP2A-B56 complexes	haploinsufficiency?	dominant-negative effect on PP2A-B56γ and B56δ complexes	haploinsufficiency: poor expression	unclear	NA
+0.4 SD	−2 SD	−3 SD	−1.6 SD	−1.9 SD	−0.8 SD	0 SD	−2 SD	NA
−3 SD	−2.3 SD	−3 SD	−1.1 SD	−4.6 SD	<−2 SD	+1.2 SD	0 SD	NA
−0.2 SD	−1.5 SD	−2 SD	−2.1 SD	−1.9 SD	−0.6	−2 SD	−1.5 SD	NA
+ (severe)	+ (mild)	+ (mild)	+ (profound)	+ (moderate)	+ (severe)	+ (mild)	+ (severe)	16/16 (100%)
+	+	−	+	NA	+	−	+	10/14 (71%)
−	−	−	−	−	−	−	−	2/16 (13%)
−	+ (ASD, ADHD)	−	−	−	−	+	+ (ASD)	7/15 (47%)
+	+	−	+	+	+	−	+ (mild)	11/16 (69%)
−	+ (NK)	−	+ (staring spells, head drops, and tonic-clonic seizures)	+ (focal epilepsy with secondary generalization)	+ (generalized tonic-clonic seizures)	−	+ (generalized tonic-clonic seizures)	10/16 (63%)
NA	NK	NA	hypsarrhythmia (West syndrome)	not specified	not specified	NA	not specified	NA
NA	3 y	NA	8 m	5 m	1 w	NA	1 y	NA
NA	ongoing	NA	ongoing	ongoing	ongoing	NA	ongoing	NA
+ (pontocerebellar hypoplasia, mild ventriculomegaly)	+ (nonspecific thinning of the corpus callosum, mild volume loss of the cerebellum)	NK	−	+ (microcephaly, enlarged subarachnoid spaces, nonspecific findings of cerebral underdevelopment)	+ (slightly dilated external and internal subarachnoid spaces, diffuse but discrete atrophy, adequate myelination)	−	+ (bilateral dilatation of perivascular spaces along the corona radiata)	10/15 (67%)
optic-nerve anomaly	NK	−	choreiform movements	−	stereotypic movements	−	−	6/15 (40%)

(*Continued on next page*)

Table 1. *Continued*

General Information	Individual 1	Individual 2	Individual 3	Individual 4	Individual 5	Individual 6	Individual 7	Individual 8
Facial								
Eyes	hypertelorism, prominent eyes	–	periorbital fullness restricted to upper eyelids, long eyelashes	ptosis, short palpebral fissures	–	prominent eyes, epicanthic folds	small palpebral fissures, deep-set eyes	megalocornea
Nose	full nasal tip, low-hanging columella	broad nasal bridge	full nasal tip	broad nasal tip	–	–	broad nasal tip	asymmetrical nostrils and bifid nasal tip
Philtrum	short philtrum	short philtrum	–	short philtrum	–	–	–	–
Other dysmorphic features	broad forehead, frontal bossing, square shape of both ears	open fontanel, plagiocephaly, some frontal bossing, prominent upper lip, sacral dimple	–	trigonocephaly, double hair whorl, high palate, low-set and anteverted ears, retrognatia	crowded teeth	plagiocephaly	broad forehead, freckling around the mouth	plagiocephaly
Other								
Extremities	single left palmar crease, long fingers and toes, bilateral sandal gap	bilateral fetal finger pads, single left palmar crease	–	poorly developed flexure fold on the third right finger, incomplete single transverse palmar crease, adducted thumbs (reducible); X-ray: ovoid appearance of vertebrae, coxa valga, slender distal phalanges	hypermobile knees	mild shortened fifth digits	–	hyperlaxity
Feeding difficulties	+	+	+	–	–	–	–	–
Vision problems	–	–	–	–	periods of sudden vision loss and pain in left eye	megalocornea, moderated excavated papillae, mild hypermetropia (both eyes +2)	NK	megalocornea, strabismus
Other	4 café-au-lait spots (max 5 mm)	–	vitamin B12 deficiency	elevated right diaphragm	recurrent ear and urinary-tract infections, heart murmur, fractures after minimal trauma	diastasis recti	frequent airway infections as a child	muscular ventricular septal defect

Abbreviations are as follows: +, present; –, not present; w, weeks; y, years; m, months; NK, not known; NA, not applicable; SD, standard deviation; DD, developmental delay; ID, intellectual disability; PDD-NOS, pervasive developmental disorder not otherwise specified; ASD, autism spectrum disorder; ADHD, attention deficit hyperactivity disorder; ESES, electrical status epilepticus during sleep; CVI, cerebral visual impairment.
[a]Additional information on variant(s) in other gene(s) is in the Supplemental Note.

microcephaly. A recognizable facial gestalt could not be observed, but some individuals showed mild dysmorphic features, such as a full nasal tip and megalocornea, and one individual had an asymmetrical face (Figure 1C). Other clinical observations included hypotonia (11/16 [69%]), feeding difficulties (9/15 [60%]), vision problems (6/14 [43%]), and congenital heart defects, the last of which included a muscular ventricular septal defect, atrial septal defect, and trileaflet aortic valve in three separate individuals.

Mutational Spectrum Is Diverse and Suggests Loss of PPP2CA Subunit Functioning

In total, 15 different *de novo* mutations in 16 individuals were identified through routine clinical diagnostic procedures, including WES (15 individuals) and microarray-based copy-number analysis (one individual; Figure 1B). The latter detected a 120 kb deletion (chr5: 133,546,961–133,667,321; GRCh37) including *PPP2CA* exon 1 and the 3′ coding region of *CDKL3* in individual 11. The variants identified by WES included a recurrent missense mutation, c.572A>G (p.His191Arg) (which is predicted to be deleterious by MutationTaster[23] and affects a highly conserved nucleotide and amino acid position in the "loop switch" of PP2A-C[24]) in individuals 1 and 6. The conformation of the loop switch determines the conformation of the active site and the binding of catalytic metal ions.[24] In addition, His191 is one of four residues forming a hydrophobic cage accommodating binding of pharmacologic PP2A inhibitors, such as okadaic acid and microcystin.[25] Gln122

Individual 9	Individual 10	Individual 11	Individual 12	Individual 13	Individual 14	Individual 15	Individual 16	Total (Percentage)
bilateral epicanthal folds	–	periorbital fulness, upslanting palpebral fissures	–	–	almond-shaped eyes	–	–	NA
–	–	–	–	–	–	broad nasal tip, small alae nasi	–	NA
–	–	–	–	–	–	–	–	NA
prominent metopic suture, mild micrognathia	–	full cheeks, thin upper lip, everted lower lip, square configuration of the lobule of the ear (right bigger than left)	high arched palate	–	small mouth, high palate	–	–	NA
bridged palmar crease, bilateral ulnar deviation of wrists and fingers, partially adducted thumbs, right hand greater than left	NK	bilateral fifth-finger clinodactyly	hyperlaxity	bilateral single palmar crease, bilateral adducted thumb	atypical single left palmar crease, pes planus, overlapping toes	single left palmar crease	–	NA
+	NK	+	+	+	+	+ (infancy)	–	9/15 (60%)
CVI	NK	immature retina at the age of 1 m	does not track or blink to threat	–	–	–	–	6/14 (43%)
mild bilateral sensorineural hearing loss	NK	inguinal hernia, umbilical hernia	constipation, atrial septal defect, low bone mineral density	trileaflet aortic valve, multiple café-au-lait macules	–	sacral haemangioma	–	NA

is another of those four residues[25] and was identified to be substituted into a histidine in individual 13 (p.Gln122His). Two other missense mutations, c.380A>G (p.Tyr127Cys) and c.794A>G (p.Tyr265Cys), affect two tyrosine residues that are within the active site and are involved in direct contacts with okadaic acid and microcystin (Tyr265)[25] and with major PP2A cellular activators, such as PTPA (Tyr127 and Tyr265)[26] and the PP2A methyltransferase LCMT-1 (Tyr127).[27] The c.391G>C (p.Asp131His) variant harbors a charge reversal in an amino acid residing nearby the "helix switch" that is directly involved in binding to LCMT-1[27] and the PP2A inhibitor TIPRL1.[28] The c.179G>T (p.Gly60Val) and c.263A>G (p.Asp88Gly) variants are in close proximity to amino acids Asp57, His59, and Asp85, which are directly involved in the binding of catalytic metal ions in the active site of PP2A-C.[25] Moreover, His59 is involved in direct binding to okadaic acid and microcystin,[25] LCMT-1,[27] and PTPA.[26] The two remaining missense variants, 667G>C (p.Asp223His) and c.668A>T (p.Asp223Val), affect an amino acid of unknown functional significance.

If not degraded by nonsense-mediated RNA decay, the frameshift c.438del (p.Phe146Leufs*29) and two of the nonsense mutations, c.373C>T (p.Gln125*) and c.640C>T (p.Arg214*), are predicted to result in severely C-terminally truncated proteins. The remaining nonsense mutation c.882dup (p.Arg295*) is located in the ultimate exon and is predicted to result in a small, 14 amino acid truncation of the Cα C-terminal tail. Importantly, this highly conserved C tail represents a focal point of PP2A regulation[29] and is reversibly modified by phosphorylation[30] and carboxymethylation[31–34] within the six most

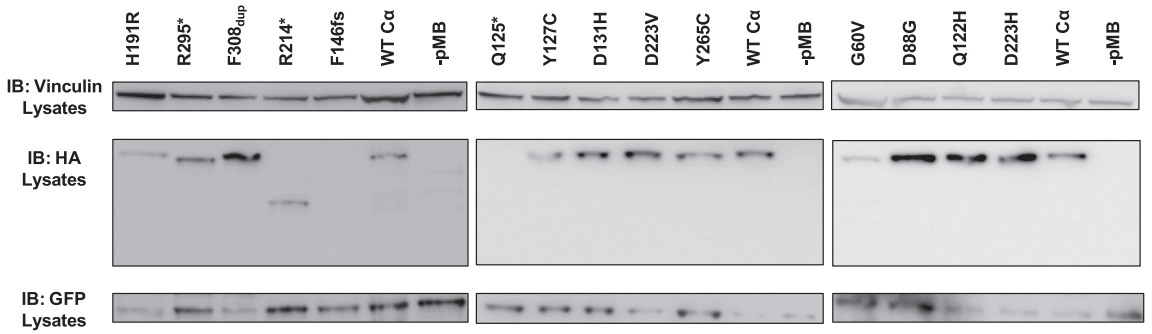

Figure 2. Levels of Mutant PP2A Cα Subunits in HEK293T Cells
HA-tagged WT and mutant Cα proteins were co-expressed with GFP (transfection control) in HEK293T cells. Protein levels were monitored in total protein lysates by immunoblotting with anti-HA and anti-GFP antibodies. Vinculin was used as a loading control. Abbreviated amino acid changes are as follows: H191R, p.His191Arg; R295*, p.Arg295*; F308dup, p.Phe308dup; R214*, p.Arg214*; F146fs, p.Phe146fs; Q125*, p.Gln125*; Y127C, p.Tyr127Cys; D131H, p.Asp131His; D223V, p.Asp223Val; Y265C, p.Tyr265Cys; G60V, p.Gly60Val; D88G, p.Asp88Gly; Q122H, p.Gln122His; and D223H, p.Asp223His.

C-terminal residues (304-T-P-D-Y-F-L-309), affecting PP2A holoenzyme assembly and activity (Figure 1B).[35–37] Interestingly, individual 4 harbors a duplication of the phenylalanine in this sequence (T-P-D-Y-F-F-L), rendering the C-tail 1 amino acid longer and possibly hindering PP2A assembly and/or activation (Figure 1B).

Population metrics based on large databases (such as the Exome Aggregation Consortium [ExAC]) Browser) indicate that, after sequence context and mutability are considered, *PPP2CA* is depleted of loss-of-function (LoF) variants according to multiple LoF metrics (pLI = 0.99; *Z* score = 4.47). Whereas these population signatures cannot be considered evidence of causality on their own, they support a hypothesis that *PPP2CA* variants leading to a functional loss are under strong purifying selection in the human population and that their occurrence could contribute to clinical phenotypes.

Both Haploinsufficiency and Non-haploinsufficiency Mechanisms Might Underlie the ID and DD Syndrome Caused by *De Novo* Variants in *PPP2CA*

We next set out to analyze both the catalytic capacity and the subunit binding of the *de novo* mutations affecting *PPP2CA*. We first attempted to determine protein levels of 14 different *de novo* mutants (one frameshift, three nonsense, one in-frame duplication, and nine missense mutants) in HEK293T cells, a frequently used model for PP2A biochemistry studies. We co-expressed the N-terminally HA-tagged Cα mutants with GFP to control for transfection efficiency. Anti-HA immunoblotting using total protein lysates of the transfected cells consistently showed the presence of protein for 12 of 14 constructs (Figure 2); that is, despite the clear presence of GFP in all conditions tested, the p.Gln125* and p.Phe146Leufs*29 mutants failed detection (Figure 2), suggesting that these mutants might not be stable. Thus, we concluded that for the p.Gln125* and p.Phe146Leufs*29 variants, haploinsufficiency is the likely underlying pathophysiological mechanism. In addition, a persistent lower protein level was seen for p.Gly60Val, leading to an inefficacy in generating reliable biochemical data. This could imply that this mutant is not stable, prompting us to advocate for a haploinsufficient mechanism in this case as well. Given the clear protein levels of all other variants examined, a dominant mechanism remained possible, and we further investigated this in additional functional assays.

PPP2CA Mutations Severely Compromise Phosphatase Activity in Most Cases

To determine intrinsic catalytic activity of the 11 Cα mutants that resulted in stable protein levels, we isolated the proteins from total lysates of transfected HEK293T cells by pull-down on HA-agarose beads and washed and incubated them with a short phospho-peptide (K-R-pT-I-R-R) for varying times (20–40 min) at 30°C, after which we used BIOMOL Green to measure the release of free phosphate. An inactive Cα mutant (p.Asp85Asn) was included as a negative control.[34] Whereas essentially no phosphatase activity was found for p.Asp85Asn, the activity of p.Gln122His, p.His191Arg, p.Asp223His, and p.Arg295* was severely decreased to 30%–50% of WT activity (Figure 3 and Table 2). In addition, PP2A activity was virtually absent for the p.Asp88Gly, p.Tyr127Cys, p.Arg214*, p.Tyr265Cys, and p.Phe308dup mutants (Figure 3). Together with the absence of the p.Gln125* and p.Phe146Leufs*29 variants and the low levels of p.Gly60Val, these results further suggest that the underlying pathophysiological mechanism is a functional loss.

On the other hand, p.Asp131His and p.Asp223Val variants displayed similar or even higher activity, indicating a divergent mechanism in these cases.

Carboxymethylation Assay Further Suggests PP2A Functional Defects

To further underscore the above activity data, we addressed potential changes in carboxymethylation of the Cα mutants by using commercially available demethyl-specific antibodies. It has previously been demonstrated that

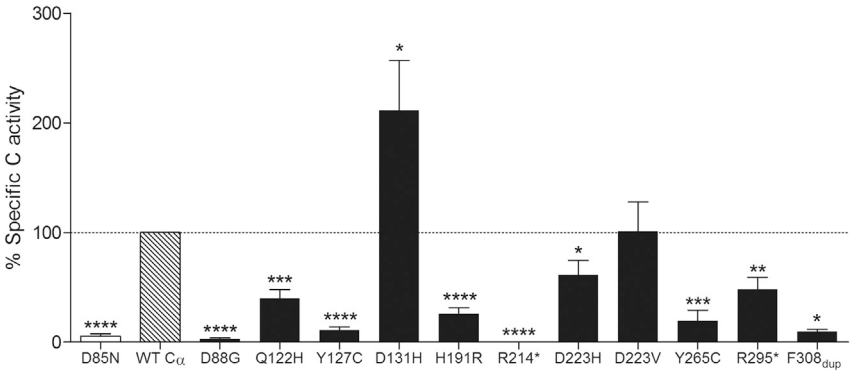

Figure 3. Phosphatase Activity of Mutant PP2A Cα Subunits

HA-tagged WT and mutant Cα proteins were purified from transfected HEK293T cells by HA pull-down, and absolute PP2A activity was determined on the K-R-pT-I-R-R phosphopeptide substrate with BIOMOL Green. Specific PP2A activities were calculated via correction of the measured activities for actual Cα inputs, determined by anti-HA immunoblotting. Results represent the average specific activity ± SEM for a given Cα mutant in relation to the specific activity of WT Cα (set at 100% in each experiment), as determined in at least three independent experiments ($n \geq 3$). A one-sample t test (compare to 100%) was used for assessing statistical significance (*$p \leq 0.05$, **$p \leq 0.01$, ***$p \leq 0.001$, ****$p \leq 0.0001$).

loss of the single C-terminal Leu309 residue is already sufficient to prevent methylation.[27,35] Hence, it is reasonable to predict that methylation of the truncated p.Arg214* and p.Arg295* mutants is no longer possible. In contrast, predicting a potential methylation defect of the p.Asp88Gly, p.Gln122His, p.Tyr127Cys, p.Asp131His, p.His191Arg, p.Asp223His, p.Asp223Val, p.Tyr265Cys, and p.Phe308dup mutants is more difficult. We therefore introduced the latter mutants, as well as WT Cα and the p.Arg295* mutant, as HA-tagged fusion proteins and subsequently assessed their methylation status in HA pull-downs.

Anti-demethyl immunoblots indicated that the p. Asp88Gly, p.Gln122His, p.Tyr127Cys, p.Asp223Val, and p.Tyr265Cys variants had lower carboxymethylation ($p = 0.001$, 0.03, 0.02, 0.03, and 0.02, respectively) than WT Cα (Figures 4A and 4B and Table 2), whereas the p.His191Arg variant showed a trend toward increased demethylation ($p = 0.095$). For the p.Asp131His and p.Asp223His variants, however, there were no significant differences ($p > 0.15$). The decrease in methylation was most pronounced for the p.Asp88Gly, p.Tyr127Cys, and p.Tyr265Cys mutants, in which the mutated residues are part of the catalytic center and are in close or direct contact with the PP2A methyltransferase LCMT-1.[27] The observed PP2A activity defects in these variants (Figure 3) are in accordance with their inability to be properly methylated, given that effective C subunit carboxymethylation requires an active conformation of PP2A-C.[27]

For the p.Phe308dup variant, the anti-demethyl antibodies revealed no signal at all, as was the case for the C tail lacking the p.Arg295* variant, suggesting that the antibodies are probably unable to recognize this mutant (Figure 4A). Hence, we could draw no conclusions regarding potential methylation defects of the variant with a 1 amino acid extension of the C tail. However, given the severe effect on activity (Figure 3), we speculate that this mutant might have impaired methylation as well.

PPP2CA Mutations Alter PP2A Subunit Binding in a Mutation-Specific Manner

To investigate whether the *PPP2CA* missense mutations affect PP2A subunit interactions, we first assessed binding of the HA-tagged Cα mutants to the endogenous A subunit. After HA pull-down of HA-tagged Cα mutants introduced in HEK293T cells, the presence of the A subunit in the bead fractions was monitored by anti-A immunoblotting. Whereas A subunit binding for the p.Gln122His, p.Tyr127Cys, p.His191Arg, p.Asp223His, and p.Asp223Val mutants was not obviously impaired in comparison with that of WT Cα, structural A subunit binding was significantly decreased for p.Asp88Gly, p.Asp131His, Tyr265Cys, p.Arg295*, and p.Phe308dup mutants (30%–60% of WT Cα binding) and even completely abolished for the p.Arg214* mutant (Figures 5A–5C and Table 2). For the latter, however, we noticed strong binding to endogenous alpha 4 (Figure 5D and Table 2), a non-canonical PP2A subunit whose binding is mutually exclusive with the A subunit. Alpha 4 binding stabilizes the C subunit in a latent form,[24,36] which is consistent with our observation of the complete lack of phosphatase activity for p.Arg214* as shown in our assays (Figure 3).

We next assessed binding of the Cα mutants to at least one representative of the regulatory B55, B56, B″, and B‴/striatin subunit classes. To this end, N-terminally GST-tagged B55α (encoded by *PPP2R2A*), B56α–B56ε (encoded by *PPP2R5A–PPP2R5E*), and B″/PR72 (encoded by *PPP2R3A*) (Figure 6A, Table 2, and Figure S1) or N-terminally GFP-tagged B‴/SG2NA (encoded by *STRN3*) (Figure 6B and Table 2) was co-expressed with HA-tagged WT or mutant Cα. The retrieved Cα proteins in GST pull-downs or GFP traps were subsequently visualized by anti-HA immunoblotting.

Whereas essentially no B-type subunit binding defects could be identified for the p.Gln122His, p.Asp233His, and p.Asp223Val variants in GST pull-downs (Figure 6C and Figures S1E–S1G), a highly diverse aberrant B-type subunit binding pattern was detected for the other mutants. The p.His191Arg mutant significantly lost binding

Table 2. Overview of Mutation-Specific Biochemical Defects

PPP2CA Variant	Protein Detected	Activity (%)	A Binding (%)	Alpha 4 Binding	Demethylation	B55α Binding (%)	B56α Binding (%)	B56β Binding (%)	B56γ1 Binding (%)	B56δ Binding (%)	B56ε Binding (%)	PR72 Binding (%)	STRN3 Binding (%)
WT Cα	+	100	100	NA	100	100	100	100	100	100	100	100	100
p.Asp88Gly	+	3****	37****	NA	1379**	0****	17****	20****	88	195	41**	18**	52**
p.Gln122His	+	40***	78	NA	183*	176	228**	177	135	285	254*	118	384*
p.Tyr127Cys	+	11****	82	NA	1109*	108	15**	27*	33*	18**	14****	31*	273
p.Asp131His	+	211*	48****	NA	200	185	0****	0****	0****	5****	0****	149	296
p.His191Arg	+	26****	102	NA	218	199	99	73	57	14****	34	65	652*
p.Asp223Val	+	101	83	NA	243*	239	165	160	254	180	163*	479	72
p.Asp233His	+	61*	81	NA	138	129	97	105	111	105	147**	108	142
p.Tyr265Cys	+	19**	30***	NA	1046*	1****	6***	3****	24*	42*	7****	2****	8****
p.Arg295*	+	48**	36**	NA	ND	0****	0****	0****	0****	18***	0*****	0****	235
p.Phe308dup	+	10***	62*	NA	ND	15***	64	166	69	206	198	5****	372*
p.Gly60Val	±	ND	ND	NA	ND	ND	ND	ND	ND	ND	ND	ND	ND
p.Gln125*	−	ND	ND	ND	ND	ND	ND	ND	ND	ND	ND	ND	ND
p.Phe146fs	−	ND	ND	ND	ND	ND	ND	ND	ND	ND	ND	ND	ND
p.Arg214*	+	0****	0****	yes	ND	0****	0****	0****	0****	0****	0****	0****	NA

Abbreviations are as follows: ND, not determinable; NA, not analyzed; +, present; ±, detected at very low level; −, not detected; *$p \leq 0.05$; *$p \leq 0.01$; ***$p \leq 0.001$; ****$p \leq 0.0001$.

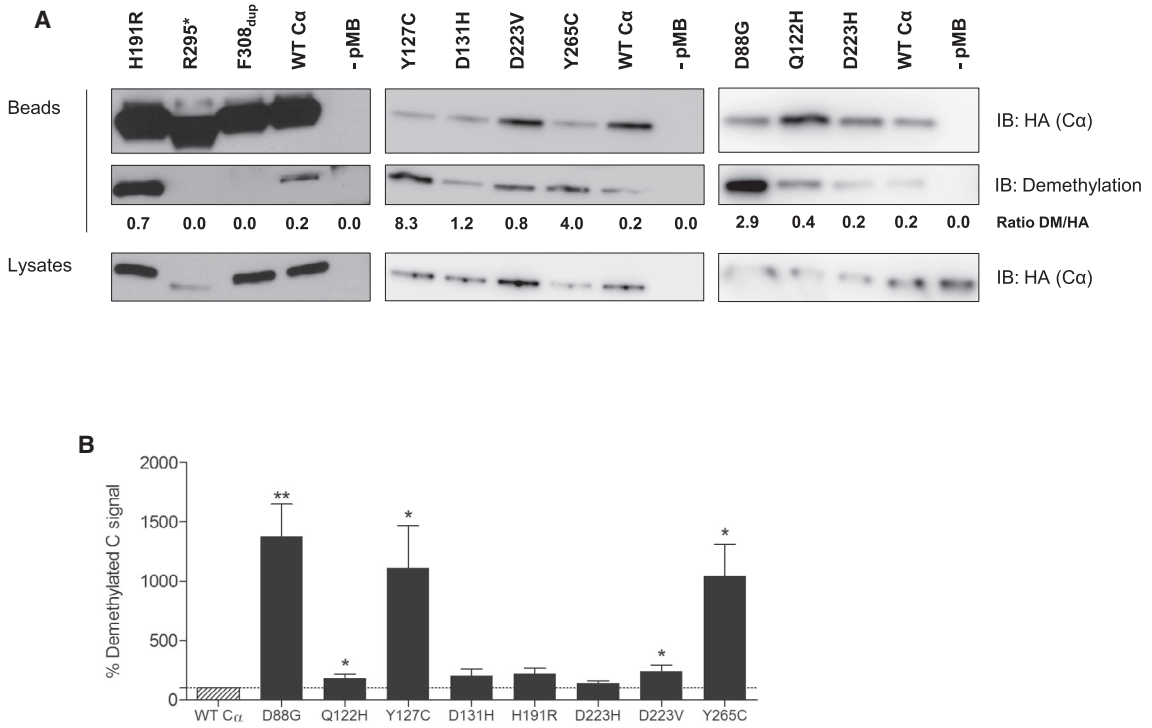

Figure 4. Carboxyterminal Methylation of Mutant PP2A Cα Subunits
(A) HA-tagged WT and mutant Cα proteins were isolated from transfected HEK293T cells by HA pull-down. PP2A C subunit methylation was subsequently assessed by immunoblotting with a demethyl-specific anti-C monoclonal antibody. Immunoblot data from a single representative experiment are shown ($n \geq 4$).
(B) The average ratios of the quantified demethyl-specific signals over the quantified anti-HA signals ± SEM are displayed ($n \geq 4$) in relation to those of WT Cα (set at 100%). A one-sample t test (compare to 100%) was used for assessing statistical significance (*$p \leq 0.05$, **$p \leq 0.01$).

to only B56δ (Figure 6C and Figure S1A). The p.Arg295* mutant lost binding to all B55, B56, and B″ subunits tested, except for B56δ, to which binding was, although significantly decreased, still slightly retained (Figure 6C and Figure S1A). The p.Asp88Gly and p.Tyr265Cys variants showed a similar pattern of severe binding defects to all B55, B56, and B″ subunits but a higher overall binding level to the B56-type subunits than p.Arg295*, particularly to the B56γ and B56δ subunits (Figure 6C and Figures S1C and S1F). The p.Asp131His variant specifically lost binding to all B56 subunits, whereas binding to B55 and B″ subunits was entirely preserved (Figure 6C and Figure S1D). On the contrary, mutant p.Phe308dup completely lost binding to B″/PR72, showed decreased binding to B55α, and retained binding to all B56 isoforms (Figure 6C and Figure S1B). For the p.Tyr127Cys variant, binding was diminished for all B56 and B″ subunits tested and intact for B55α (Figures 6A and 6C). As expected from its complete lack of A subunit binding, p.Arg214* failed to bind any B-type subunit tested (data not shown).

Interestingly, the majority of Cα mutants retained binding to the B‴/striatin subunit STRN3, and for the p.Gln122His, p.His191Arg, and p.Phe308dup variants, this interaction was even significantly enhanced (Figures 6B and 6C). This observation was also previously made for ID-associated mutations in *PPP2R1A*, encoding the Aα subunit.[38] However, for the p.Asp88Gly and p.Tyr265Cys mutants, STRN3 binding was diminished or completely abolished (Figures 6B and 6C).

Discussion

PP2A is an important holoenzyme for which broad substrate specificity is orchestrated by different subunit compositions: in particular, the B subunits play a pivotal role in determining substrate specificity, regulation, and hence physiologic functions of the different PP2A complexes. With this broad specificity, PP2A is involved in diverse cellular processes, and variants in either of these subunits could therefore cause disease. Here, we report the identification of a syndrome caused by *de novo* mutations in *PPP2CA* and characterized by mild to profound ID and DD, behavioral problems, variable types of epilepsy, hypotonia, abnormal head circumference, and brain abnormalities such as corpus callosum abnormalities and ventriculomegaly. Some individuals had mild dysmorphic features, but a recognizable facial gestalt could not be observed.

Mutations in several other PP2A-subunit-encoding genes have been reported before and result in an ID and DD phenotype. Interestingly, albeit not unsurprisingly,

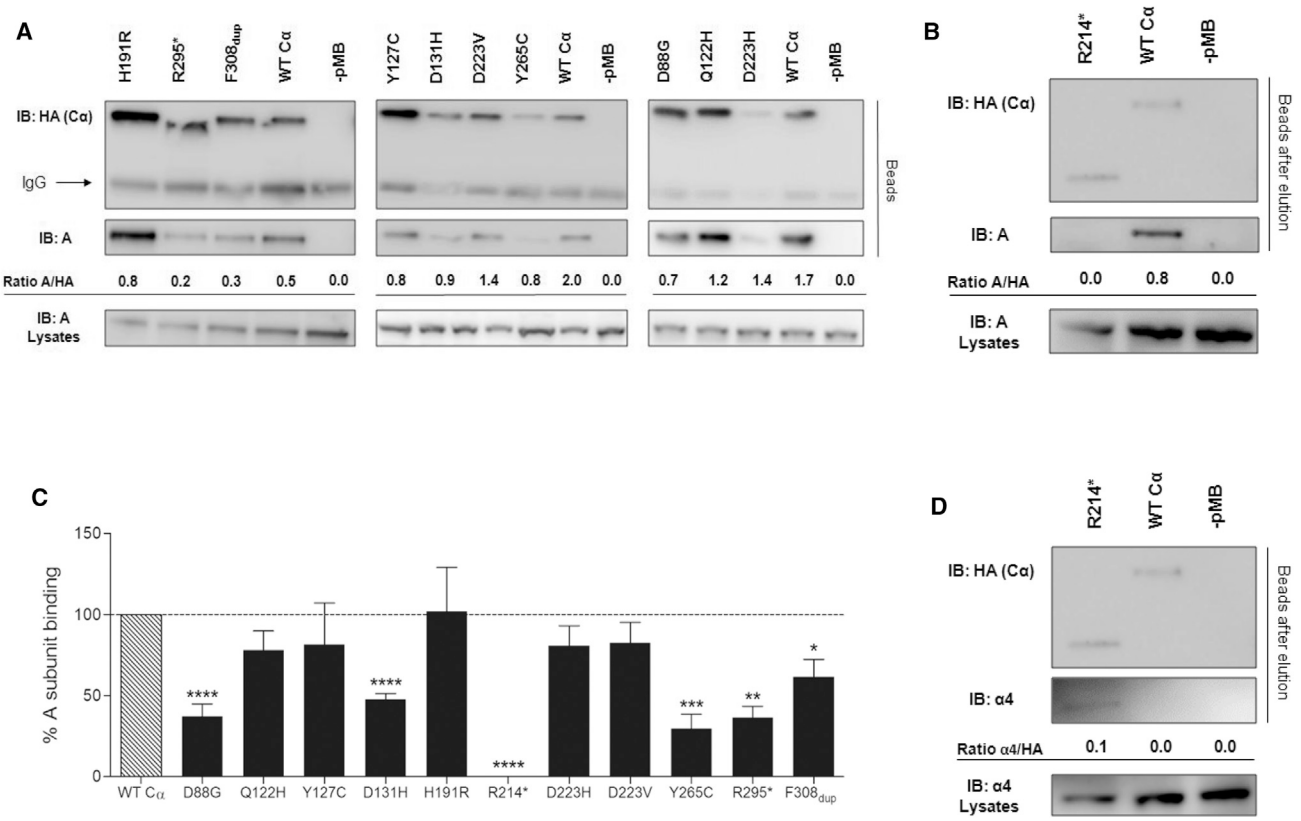

Figure 5. Binding of Mutant PP2A Cα Subunits to the A Subunit

(A) A subunit binding. HA-tagged WT and mutant Cα proteins were purified from transfected HEK293T cells by HA pull-down, and the presence of endogenous A subunit in the complexes was determined by anti-A immunoblotting. Abbreviated amino acid changes are as follows: H191R, p.His191Arg; R295*, p.Arg295*; F308dup, p.Phe308dup; Y127C, p.Tyr127Cys; D131H, p.Asp131His; D223V, p.Asp223Val; Y265C, p.Tyr265Cys; D88G, p.Asp88Gly; Q122H, p.Gln122His; and D223H, p.Asp223His.

(B) Same experimental setup as in (A), but in this case, HA-agarose-bound proteins were eluted from the beads with an excess of free HA-tagged peptide before anti-A immunoblotting of the eluates. This setup was necessary for enabling unambiguous visualization of HA-tagged p.Arg214*, which co-migrated with immunoglobulin light chains at approximately 25 kDa.

(C) Quantified values of A subunit binding. Results represent the average value ± SEM of the ratios of the quantified anti-A signal to the quantified anti-HA signal for a given Cα mutant in relation to those of WT Cα (set at 100% in each experiment), as determined in at least four independent experiments ($n \geq 4$). A one-sample t test (compare to 100%) was used for assessing statistical significance (*$p \leq 0.05$, **$p \leq 0.01$, ***$p \leq 0.001$, ****$p \leq 0.0001$).

(D) Alpha 4 subunit binding. HA-tagged WT and p.Arg214* mutant Cα proteins were purified from transfected HEK293T cells by HA pull-down and eluted from the beads by excess HA peptide, and eluates were subjected to immunoblotting with anti-alpha 4 monoclonal antibodies for the detection of binding of endogenous alpha 4.

individuals with a *de novo* mutation in *PPP2CA* showed a phenotypic resemblance to those individuals harboring an ID- and DD-related pathogenic variant in other PP2A subunits[10–12] (Table S2). This overlap consisted of ID, DD, and hypotonia (in all individuals with *PPP2R1A* and *PPP2R5D* mutations), epilepsy and ventriculomegaly (in some individuals with *PPP2R1A* and *PPP2R5D* mutations), ASD (in some individuals with a *PPP2R5D* mutation), corpus callosum agenesis (in all individuals with a *PPP2R1A* mutation and some individuals with a *PPP2R5D* mutation), and congenital heart disease (ventricular and atrial septal defects in two individuals with a mutation in *PPP2R5D*). Severe speech delay was also noted in multiple individuals and for multiple subunits, which might be partially related to the severity of ID but was more severe than expected in several individuals. A noticeable difference from mutations in other subunits is the absence of overgrowth, which was reported for individuals with pathogenic mutations in *PPP2R5B*, *PPP2R5C*, and *PPP2R5D*[11] but was observed in only one individual with a *de novo* mutation in *PPP2CA*. In addition, although two individuals were macrocephalic, five other individuals had microcephaly, a phenotype also reported for cases of *PPP2R1A* mutations.[10] Recently, brain-specific *Ppp2ca* knockout was reported to result in mice with obvious morphological and behavioral abnormalities, including microcephaly, cortical neuronal atrophy, plastic synapse deficits, and learning and memory impairments at an early postnatal stage.[39] These features were also partly observed in individuals with *de novo* mutations in *PPP2CA*, and although the phenotypes of the heterozygous mice (if any) were not further documented, these mice could be an excellent *in vivo* model for further studies. Likewise, congenital heart defects, specifically affecting septum

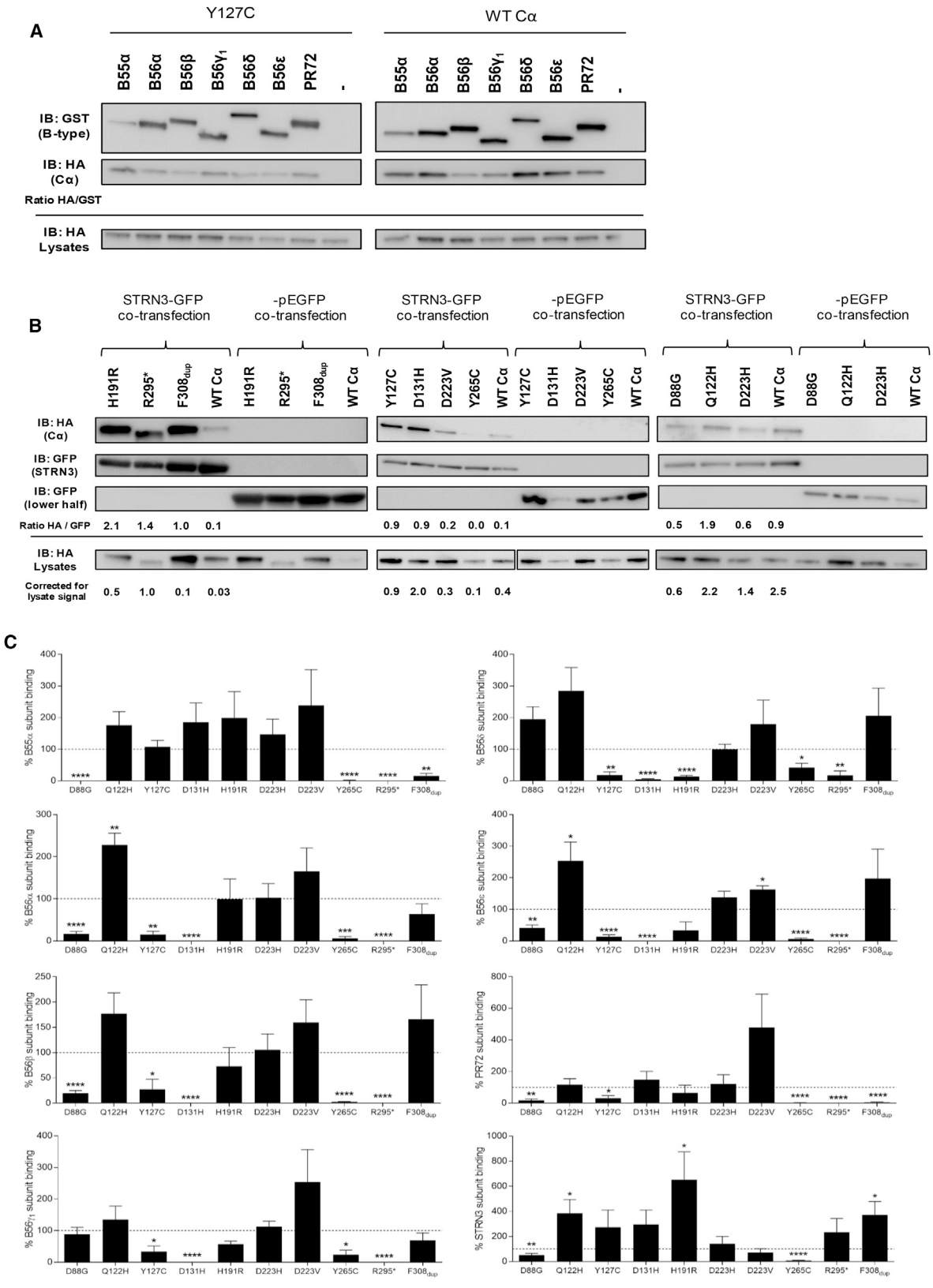

Figure 6. Binding of Mutant PP2A Cα Subunits to B-type Subunits

(A) GST-tagged B-type subunits were co-expressed with HA-tagged WT or mutant p.Tyr127Cys Cα protein in HEK293T cells. The presence of the PP2A C variant was subsequently assessed in GST pull-downs by anti-HA immunoblotting. Representative blots of similar assays with other Cα variants can be found in Figure S1.

(B) GFP-tagged B‴/STRN3 or GFP alone was co-expressed with HA-tagged WT or mutant Cα proteins in HEK293T cells. The presence of Cα variants was subsequently assessed in GFP traps by anti-HA immunoblotting.

(legend continued on next page)

formation, have been reported in B56γ-knockout mice and in transgenic mice specifically overexpressing a dominant-negative mutant of Aα in (cardiac) muscle.[40,41] All functionally characterized and clinically described variants in subunits of PP2A so far and our data on *PPP2CA* variants collectively seem to constitute overlapping syndromic forms of ID involving more than one gene but functionally converging to PP2A deficiency, and they could therefore be redefined as "PP2A-related neurodevelopmental syndrome."

Notably, for most individuals, WES was used to identify the *PPP2CA* mutation, so other rare (*de novo*) mutations were also identified in 6 of 16 individuals. Whereas these most likely reflect the background per-generation *de novo* mutation rate, a contribution of these *de novo* variants to the individuals' phenotypes cannot be excluded. Similarly, involvement of the partial *CDKL3* deletion to the phenotype of individual 11 cannot be ruled out given that a balanced *CDKL3*-disrupting translocation leading to decreased expression of *CDKL3* has previously been reported in an individual with mild ID.[42] To collect further insight into the clinical spectrum, we established a website on the Human Disease Genes platform for the collection of clinical data (see Web Resources).

By far most reported individuals with PP2A variants so far harbor *de novo* mutations in *PPP2R5D*, encoding the regulatory B56δ subunit.[10–12] Biochemical characterization has revealed that the vast majority of these variants show decreased binding to the A and C subunits, hinting at a dominant-negative mode of action.[10] Similarly, characterization of *de novo* mutations in *PPP2R1A*, encoding the scaffolding Aα subunit,[10] has identified defective binding of nearly all B-type subunits, except for B56δ. Yet for the latter variants, the Aα-B56δ complexes have proved catalytically impaired,[10] potentially because of increased recruitment of a cellular PP2A inhibitor, TIPRL1.[38] Our functional assays, focusing on the functional defects following *PPP2CA* mutations, showed similar defects—that is, our binding assays suggested that some Cα variants, although catalytically impaired, were indeed still able to form trimeric complexes with specific B-type subunits, providing a mechanistic basis for their potential dominant-negative mode of action. Clearly, such a dominant-negative mechanism would affect only a set of specific holoenzymes rather than the whole PP2A spectrum. This scenario is most likely the case for the p.Asp88Gly, p.Tyr265Cys, p.Arg295*, and p.Phe308dup variants, which all showed significantly decreased catalytic activity but still retained binding to at least B56δ. Moreover, the p.Asp88Gly and p.Arg295* variants occurred in individuals with severe ID, and the p.Phe308dup variant caused moderate ID—all in line with a potential dominant-negative effect on PP2A-B56δ complexes (for p.Arg295*), on PP2A-B56γ and B56δ complexes (for p.Asp88Gly), or on all PP2A-B56 complexes (for p.Phe308dup). In contrast, the individual with the p.Tyr265Cys variant had mild ID (with comorbid epilepsy, hypotonia, brain MRI abnormalities, ASD, and ADHD), suggesting that in this case, the 50% retained binding to B56δ might not be causally involved, but rather the significantly decreased binding to all B-type subunits is the most important determinant, bringing us into a scenario of haploinsufficiency in this particular individual. Likewise, haploinsufficiency would be the proposed mechanism for the partial *PPP2CA* deletion and the p.Gln125*, p.Phe146Leufs*29, and p.Arg214* variants, all of which lead to complete null alleles (due to the lack of expression in the first three cases or expression of a completely dysfunctional variant in the last case), as well as for the very poorly expressed p.Gly60Val variant. All of these individuals had mild ID often accompanied by severe epilepsy. Notably, the remaining 50% of WT Cα in those five individuals might no longer be sufficient to assemble all PP2A holoenzymes, as previously suggested for specific cancer-associated Aα (*PPP2R1A*) mutants[43,44] and haploinsufficiency of *PPP2R4*, encoding the PP2A activator PTPA.[45] Upon loss of one functional allele for those two genes, selective PP2A dysfunctions were observed for B56-subunit-containing complexes, specifically B56γ, B56δ, and B56ε (whereas B55 complexes remained fully functional), as a result of a competition mechanism between B subunits for binding the remaining WT Aα subunit or fully activated C subunit. In other words, both *PPP2R1A* and *PPP2R4* haploinsufficiency caused a selective PP2A-B56 defect. In this respect, it is interesting to point out that three B-type-subunit-encoding genes hitherto reported to be involved in the etiology of ID and DD all encode subunits of the B56 family (δ, γ, and β isoforms).[10,11] Thus, in those *PPP2CA* cases where we suspect haploinsufficiency as the pathological mechanism, the eventual PP2A dysfunctions could be highly similar and mainly affect B56-type holoenzymes. On the basis of our biochemical assays, such a selective B56 defect also seems to be the case for the catalytically competent p.Asp131His variant, which retained binding to all B-type subunits tested, except for all B56 isoforms. The p.Tyr127Cys variant also lost binding to all B56 subunits, as well as to B″/PR72. However, in this case, the catalytic activity and methylation of this variant were also significantly impaired, suggesting that a dominant-negative mechanism toward PP2A-B55 and PP2A-STRN

(C) Quantified values of C subunit binding. Results represent the average value ± SEM of the ratios of the quantified anti-HA signal to the quantified anti-GST or anti-GFP (in the case of STRN3) signal for a given Cα mutant in relation to those of WT Cα (set at 100% in each experiment, dotted line), as determined in at least three independent binding experiments ($n \geq 3$). A one-sample t test (compare to 100%) was used for assessing statistical significance (*$p \leq 0.05$, **$p \leq 0.01$, ***$p \leq 0.001$, ****$p \leq 0.0001$).
Abbreviated amino acid changes are as follows: H191R, p.His191Arg; R295*, p.Arg295*; F308dup, p.Phe308dup; Y265C, p.Tyr265Cys; Y127C, p.Tyr127Cys; D131H, p.Asp131His; D223V, p.Asp223Val; D88G, p.Asp88Gly; Q122H, p.Gln122His; and D223H, p.Asp223His.

complexes might additionally be in place—further explaining the severe ID in this individual. Despite a relatively large number of available *PPP2CA*-knockout mouse models, heterozygous Cα-null mice have unfortunately never been phenotypically or biochemically examined.[46] In any case, our data provide evidence that *PPP2CA* is a haploinsufficient gene in humans.

The only recurrent *PPP2CA* variant in our cohort, c.572A>G (p.His191Arg), showed a (non-significant) increase in demethylation signal (218%; $p = 0.095$) and a decrease in activity (48%; $p = 0.001$), whereas no changes in A or B subunit interaction could be detected, except for B56δ (for which binding was decreased) and for B‴/STRN3 (for which binding was increased). Both individuals with this variant had a mild ID phenotype and fever-related seizures. Structural studies suggested that the His191 residue is important in PP2A-C's interaction with alpha 4[24] and thereby induces displacement of the catalytic center and subsequent reduction in activity.[28] Additionally, in a yeast model, the p.His191Arg variant was incapable of exhibiting a dominant-negative effect on WT human PP2A Cα in a growth assay.[47] This could indicate a potential haploinsufficient mechanism of the p.His191Arg variant, which mainly affects B56δ-containing holoenzymes. The biochemical profile of the p.Gln122His variant appeared very similar to that of p.His191Arg, except for the retained binding to B56δ in p.Gln122His. Both affected residues are indeed two of four residues that are directly involved in binding the hydrophobic part of pharmacologic PP2A inhibitors, okadaic acid, and microcystin.[25]

Finally, the p.Asp223His and p.Asp223Val variants did not seem to have a significant impact on PP2A assembly and function in any of our assays tested, except for a slight increase in B56ε binding (150%), a slight decrease in activity (for p.Asp223His), and a light increase in demethylation signal (for p.Asp223Val). The latter might suggest that the clinical phenotype might be milder, but this was not the case for individual 16 (p.Asp223His), who had severe ID. Also, although the other individual (individual 7, p.Asp223Val) initially had a normal IQ, she showed speech delay and ASD and additionally developed progressive cognitive dysfunction after a psychotic episode at the age of 17 years. In the absence of a clear pathogenic effect for these two variants in the majority of our biochemical assays tested, it could be speculated that another (yet unidentified) genetic variant contributes to the disease manifestation of individuals 7 and 16.

Many of the observed biochemical defects in specific Cα variants can be rationalized by structural data from crystallographic studies or are sustained by previously reported biochemical and functional studies of PP2A C mutants in yeast. The variants affecting Asp88 and two tyrosine residues in the catalytic center—p.Tyr127Cys and p.Tyr265Cys—both induced a drastic decrease in methylation and activity. Most likely the variants induce an inactive Cα conformation, which subsequently prevents methylation. In yeast, a p.Tyr127Asn variant was also identified as LoF because it could not rescue the growth defect of a PP2A-C deletion strain.[47] For the p.Asp131His, p.His191Arg, and p.Asp223His variants, the effects were less clear, although there might have been a trend toward slightly decreased methylation for the pHis191Arg variant. On the other hand, a slight but significant decrease in methylation of the p.Asp223Val mutant was detected, whereas the p.Asp223His variant, affected in the same residue, behaved like the WT. Besides a charge difference between the mutated amino acids, a straightforward structural explanation for this observation could not be found. A similar increase in demethylated signal could be observed for the p.Gln122His variant. Although it's impossible to measure with the available antibodies, we expect methylation of p.Phe308dup to be diminished as well. On the basis of the "deep and narrow cleft" conformation of the active center of the PP2A methyltransferase LCMT-1 and the fact that several residues in the C tail need to form stabilizing contacts with the LCMT-1 active-site residues for efficient methylation to occur, a tail that is 1 amino acid too long might no longer fit in and thus no longer be modified.

The c.640 C>T (p.Arg214*) nonsense mutation is located in *PPP2CA* exon 5. Migueleti et al. reported on the existence of a shorter *PPP2CA* mRNA, in which this specific exon can be skipped, in peripheral-blood mononuclear cells under specific growth conditions (serum exhaustion), and this mRNA resulted in a slightly shorter Cα isoform.[48] Although we do not favor potential exon 5 skipping in the c.640 C>T (p.Arg214*) variant given our data and observed molecular weight of the protein detected, it is remarkable that this shorter isoform was reported as catalytically inactive without any binding to the scaffolding A subunit and increased binding to alpha 4, very much like our data for the truncated p.Arg214* protein. This would suggest an important role for exon-5-encoded amino acids in A subunit binding. Tang et al. further demonstrated that expression of the shorter Cα isoform had no effect on the expression or the modification of the longer Cα variant, thus disfavoring a dominant-negative effect of the shorter variant.[49]

In summary, we have identified 16 individuals with a syndrome characterized by ID, DD, hypotonia, epilepsy, behavioral problems, and structural abnormalities of the brain and with a *de novo* mutation in or partial deletion of *PPP2CA*, encoding one of the catalytic subunits of PP2A. Functional characterization of all the Cα variants in HEK293T cells showed a diverse spectrum of biochemical distortions that were unique to each variant but always justified the conclusion of a functional loss and affected at least the functionality of the PP2A-B56δ complexes. Only for both p.Asp223 missense variants, our results failed to reveal a major biochemical defect. Our data further expand the repertoire of PP2A subunits involved in the etiology of ID and DD and underscore

the importance of PP2A in neurodevelopmental processes and brain function. Hence, we propose that *de novo* mutations in *PPP2CA*, *PPP2R1A*, and *PPP2R5D* constitute a spectrum of overlapping ID syndromes characterized by mild to severe phenotypes and functional convergence by severe PP2A dysfunction, and we propose that these collectively be called "PP2A-related neurodevelopmental disorders."

Supplemental Data

Supplemental Data include a Supplemental Note, one figure, and two tables and can be found with this article online at https://doi.org/10.1016/j.ajhg.2018.12.002.

Acknowledgments

The authors thank the individuals and their parents for participating in the study. Funding was provided by the IAP program of the Belgian federal government (P7/13 to V.J.), Research Foundation-Flanders (to V.J.), and the University of Leuven (C24/17/073 to V.J.). S.R. received an FWO-SB fellowship from the Research Foundation-Flanders. D.H. received a fellowship of the Flemish Agency for Innovation by Science and Technology. This work was financially supported by grants from the Netherlands Organization for Health Research and Development (917-86-319 and 912-12-109 to B.B.A.d.V.) and made use of data generated by the DECIPHER Consortium. A full list of centers who contributed to the generation of the data is available at https://decipher.sanger.ac.uk/ and via email at decipher@sanger.ac.uk. Funding for the project was provided by the Wellcome Trust.

Declaration of Interests

H.M.L. is an employee of GeneDx Inc., a wholly owned subsidiary of OPKO Health Inc.

Received: June 6, 2018
Accepted: December 6, 2018
Published: December 27, 2018

Web Resources

DECIPHER, https://decipher.sanger.ac.uk/
denovo-db, http://denovo-db.gs.washington.edu/denovo-db/
ExAC Browser, http://exac.broadinstitute.org/
GeneMatcher, https://genematcher.org/
Human Disease Genes: PPP2CA, http://www.humandiseasegenes.com/PPP2CA/
OMIM, http://www.omim.org/

References

1. Vissers, L.E., Gilissen, C., and Veltman, J.A. (2016). Genetic studies in intellectual disability and related disorders. Nat. Rev. Genet. *17*, 9–18.
2. Deciphering Developmental Disorders, S.; and Deciphering Developmental Disorders Study (2015). Large-scale discovery of novel genetic causes of developmental disorders. Nature *519*, 223–228.
3. de Ligt, J., Willemsen, M.H., van Bon, B.W., Kleefstra, T., Yntema, H.G., Kroes, T., Vulto-van Silfhout, A.T., Koolen, D.A., de Vries, P., Gilissen, C., et al. (2012). Diagnostic exome sequencing in persons with severe intellectual disability. N. Engl. J. Med. *367*, 1921–1929.
4. Gilissen, C., Hehir-Kwa, J.Y., Thung, D.T., van de Vorst, M., van Bon, B.W., Willemsen, M.H., Kwint, M., Janssen, I.M., Hoischen, A., Schenck, A., et al. (2014). Genome sequencing identifies major causes of severe intellectual disability. Nature *511*, 344–347.
5. Rauch, A., Wieczorek, D., Graf, E., Wieland, T., Endele, S., Schwarzmayr, T., Albrecht, B., Bartholdi, D., Beygo, J., Di Donato, N., et al. (2012). Range of genetic mutations associated with severe non-syndromic sporadic intellectual disability: an exome sequencing study. Lancet *380*, 1674–1682.
6. Lelieveld, S.H., Reijnders, M.R., Pfundt, R., Yntema, H.G., Kamsteeg, E.J., de Vries, P., de Vries, B.B., Willemsen, M.H., Kleefstra, T., Löhner, K., et al. (2016). Meta-analysis of 2,104 trios provides support for 10 new genes for intellectual disability. Nat. Neurosci. *19*, 1194–1196.
7. Deciphering Developmental Disorders Study (2017). Prevalence and architecture of de novo mutations in developmental disorders. Nature *542*, 433–438.
8. Turner, T.N., Hormozdiari, F., Duyzend, M.H., McClymont, S.A., Hook, P.W., Iossifov, I., Raja, A., Baker, C., Hoekzema, K., Stessman, H.A., et al. (2016). Genome sequencing of autism-affected families reveals disruption of putative noncoding regulatory DNA. Am. J. Hum. Genet. *98*, 58–74.
9. Perucca, P., Scheffer, I.E., Harvey, A.S., James, P.A., Lunke, S., Thorne, N., Gaff, C., Regan, B.M., Damiano, J.A., Hildebrand, M.S., et al. (2017). Real-world utility of whole exome sequencing with targeted gene analysis for focal epilepsy. Epilepsy Res. *131*, 1–8.
10. Houge, G., Haesen, D., Vissers, L.E., Mehta, S., Parker, M.J., Wright, M., Vogt, J., McKee, S., Tolmie, J.L., Cordeiro, N., et al. (2015). B56δ-related protein phosphatase 2A dysfunction identified in patients with intellectual disability. J. Clin. Invest. *125*, 3051–3062.
11. Loveday, C., Tatton-Brown, K., Clarke, M., Westwood, I., Renwick, A., Ramsay, E., Nemeth, A., Campbell, J., Joss, S., Gardner, M., et al.; Childhood Overgrowth Collaboration (2015). Mutations in the PP2A regulatory subunit B family genes PPP2R5B, PPP2R5C and PPP2R5D cause human overgrowth. Hum. Mol. Genet. *24*, 4775–4779.
12. Shang, L., Henderson, L.B., Cho, M.T., Petrey, D.S., Fong, C.T., Haude, K.M., Shur, N., Lundberg, J., Hauser, N., Carmichael, J., et al. (2016). De novo missense variants in PPP2R5D are associated with intellectual disability, macrocephaly, hypotonia, and autism. Neurogenetics *17*, 43–49.
13. Janssens, V., and Goris, J. (2001). Protein phosphatase 2A: a highly regulated family of serine/threonine phosphatases implicated in cell growth and signalling. Biochem. J. *353*, 417–439.
14. Cundell, M.J., Hutter, L.H., Nunes Bastos, R., Poser, E., Holder, J., Mohammed, S., Novak, B., and Barr, F.A. (2016). A PP2A-B55 recognition signal controls substrate dephosphorylation kinetics during mitotic exit. J. Cell Biol. *214*, 539–554.
15. Hertz, E.P.T., Kruse, T., Davey, N.E., López-Méndez, B., Sigurðsson, J.O., Montoya, G., Olsen, J.V., and Nilsson, J. (2016). A conserved motif provides binding specificity to the PP2A-B56 phosphatase. Mol. Cell *63*, 686–695.

16. Lambrecht, C., Haesen, D., Sents, W., Ivanova, E., and Janssens, V. (2013). Structure, regulation, and pharmacological modulation of PP2A phosphatases. Methods Mol. Biol. *1053*, 283–305.
17. Backx, L., Vermeesch, J., Pijkels, E., de Ravel, T., Seuntjens, E., and Van Esch, H. (2010). PPP2R2C, a gene disrupted in autosomal dominant intellectual disability. Eur. J. Med. Genet. *53*, 239–243.
18. Graham, J.M., Jr., Wheeler, P., Tackels-Horne, D., Lin, A.E., Hall, B.D., May, M., Short, K.M., Schwartz, C.E., and Cox, T.C. (2003). A new X-linked syndrome with agenesis of the corpus callosum, mental retardation, coloboma, micrognathia, and a mutation in the Alpha 4 gene at Xq13. Am. J. Med. Genet. A. *123A*, 37–44.
19. Trockenbacher, A., Suckow, V., Foerster, J., Winter, J., Krauss, S., Ropers, H.H., Schneider, R., and Schweiger, S. (2001). MID1, mutated in Opitz syndrome, encodes an ubiquitin ligase that targets phosphatase 2A for degradation. Nat. Genet. *29*, 287–294.
20. Esmaeeli-Nieh, S., Fenckova, M., Porter, I.M., Motazacker, M.M., Nijhof, B., Castells-Nobau, A., Asztalos, Z., Weißmann, R., Behjati, F., Tzschach, A., et al. (2016). BOD1 is required for cognitive function in humans and Drosophila. PLoS Genet. *12*, e1006022.
21. Porter, I.M., Schleicher, K., Porter, M., and Swedlow, J.R. (2013). Bod1 regulates protein phosphatase 2A at mitotic kinetochores. Nat. Commun. *4*, 2677.
22. Sobreira, N., Schiettecatte, F., Valle, D., and Hamosh, A. (2015). GeneMatcher: a matching tool for connecting investigators with an interest in the same gene. Hum. Mutat. *36*, 928–930.
23. Schwarz, J.M., Cooper, D.N., Schuelke, M., and Seelow, D. (2014). MutationTaster2: mutation prediction for the deep-sequencing age. Nat. Methods *11*, 361–362.
24. Jiang, L., Stanevich, V., Satyshur, K.A., Kong, M., Watkins, G.R., Wadzinski, B.E., Sengupta, R., and Xing, Y. (2013). Structural basis of protein phosphatase 2A stable latency. Nat. Commun. *4*, 1699.
25. Xing, Y., Xu, Y., Chen, Y., Jeffrey, P.D., Chao, Y., Lin, Z., Li, Z., Strack, S., Stock, J.B., and Shi, Y. (2006). Structure of protein phosphatase 2A core enzyme bound to tumor-inducing toxins. Cell *127*, 341–353.
26. Guo, F., Stanevich, V., Wlodarchak, N., Sengupta, R., Jiang, L., Satyshur, K.A., and Xing, Y. (2014). Structural basis of PP2A activation by PTPA, an ATP-dependent activation chaperone. Cell Res. *24*, 190–203.
27. Stanevich, V., Jiang, L., Satyshur, K.A., Li, Y., Jeffrey, P.D., Li, Z., Menden, P., Semmelhack, M.F., and Xing, Y. (2011). The structural basis for tight control of PP2A methylation and function by LCMT-1. Mol. Cell *41*, 331–342.
28. Wu, C.G., Zheng, A., Jiang, L., Rowse, M., Stanevich, V., Chen, H., Li, Y., Satyshur, K.A., Johnson, B., Gu, T.J., et al. (2017). Methylation-regulated decommissioning of multimeric PP2A complexes. Nat. Commun. *8*, 2272.
29. Janssens, V., Longin, S., and Goris, J. (2008). PP2A holoenzyme assembly: in cauda venenum (the sting is in the tail). Trends Biochem. Sci. *33*, 113–121.
30. Schmitz, M.H., Held, M., Janssens, V., Hutchins, J.R., Hudecz, O., Ivanova, E., Goris, J., Trinkle-Mulcahy, L., Lamond, A.I., Poser, I., et al. (2010). Live-cell imaging RNAi screen identifies PP2A-B55alpha and importin-beta1 as key mitotic exit regulators in human cells. Nat. Cell Biol. *12*, 886–893.
31. De Baere, I., Derua, R., Janssens, V., Van Hoof, C., Waelkens, E., Merlevede, W., and Goris, J. (1999). Purification of porcine brain protein phosphatase 2A leucine carboxyl methyltransferase and cloning of the human homologue. Biochemistry *38*, 16539–16547.
32. Lee, J., Chen, Y., Tolstykh, T., and Stock, J. (1996). A specific protein carboxyl methylesterase that demethylates phosphoprotein phosphatase 2A in bovine brain. Proc. Natl. Acad. Sci. USA *93*, 6043–6047.
33. Lee, J., and Stock, J. (1993). Protein phosphatase 2A catalytic subunit is methyl-esterified at its carboxyl terminus by a novel methyltransferase. J. Biol. Chem. *268*, 19192–19195.
34. Ogris, E., Du, X., Nelson, K.C., Mak, E.K., Yu, X.X., Lane, W.S., and Pallas, D.C. (1999). A protein phosphatase methylesterase (PME-1) is one of several novel proteins stably associating with two inactive mutants of protein phosphatase 2A. J. Biol. Chem. *274*, 14382–14391.
35. Longin, S., Zwaenepoel, K., Louis, J.V., Dilworth, S., Goris, J., and Janssens, V. (2007). Selection of protein phosphatase 2A regulatory subunits is mediated by the C terminus of the catalytic Subunit. J. Biol. Chem. *282*, 26971–26980.
36. Sents, W., Ivanova, E., Lambrecht, C., Haesen, D., and Janssens, V. (2013). The biogenesis of active protein phosphatase 2A holoenzymes: a tightly regulated process creating phosphatase specificity. FEBS J. *280*, 644–661.
37. Löw, C., Quistgaard, E.M., Kovermann, M., Anandapadamanaban, M., Balbach, J., and Nordlund, P. (2014). Structural basis for PTPA interaction with the invariant C-terminal tail of PP2A. Biol. Chem. *395*, 881–889.
38. Haesen, D., Abbasi Asbagh, L., Derua, R., Hubert, A., Schrauwen, S., Hoorne, Y., Amant, F., Waelkens, E., Sablina, A., and Janssens, V. (2016). Recurrent PPP2R1A mutations in uterine cancer act through a dominant-negative mechanism to promote malignant cell growth. Cancer Res. *76*, 5719–5731.
39. Liu, B., Sun, L.H., Huang, Y.F., Guo, L.J., and Luo, L.S. (2018). Protein phosphatase 2ACα gene knock-out results in cortical atrophy through activating hippo cascade in neuronal progenitor cells. Int. J. Biochem. Cell Biol. *95*, 53–62.
40. Varadkar, P., Despres, D., Kraman, M., Lozier, J., Phadke, A., Nagaraju, K., and Mccright, B. (2014). The protein phosphatase 2A B56γ regulatory subunit is required for heart development. Dev. Dyn. *243*, 778–790.
41. Brewis, N., Ohst, K., Fields, K., Rapacciuolo, A., Chou, D., Bloor, C., Dillmann, W., Rockman, H., and Walter, G. (2000). Dilated cardiomyopathy in transgenic mice expressing a mutant A subunit of protein phosphatase 2A. Am. J. Physiol. Heart Circ. Physiol. *279*, H1307–H1318.
42. Dubos, A., Pannetier, S., and Hanauer, A. (2008). Inactivation of the CDKL3 gene at 5q31.1 by a balanced t(X;5) translocation associated with nonspecific mild mental retardation. Am. J. Med. Genet. A. *146A*, 1267–1279.
43. Chen, W., Arroyo, J.D., Timmons, J.C., Possemato, R., and Hahn, W.C. (2005). Cancer-associated PP2A Aalpha subunits induce functional haploinsufficiency and tumorigenicity. Cancer Res. *65*, 8183–8192.
44. Ruediger, R., Ruiz, J., and Walter, G. (2011). Human cancer-associated mutations in the Aα subunit of protein phosphatase 2A increase lung cancer incidence in Aα knock-in and knockout mice. Mol. Cell. Biol. *31*, 3832–3844.
45. Sents, W., Meeusen, B., Kalev, P., Radaelli, E., Sagaert, X., Miermans, E., Haesen, D., Lambrecht, C., Dewerchin, M., Carmeliet, P., et al. (2017). PP2A inactivation mediated by *PPP2R4*

haploinsufficiency promotes cancer development. Cancer Res. *77*, 6825–6837.
46. Reynhout, S., and Janssens, V. (2019). Physiologic functions of PP2A: Lessons from genetically modified mice. Biochim Biophys Acta Mol Cell Res *1866*, 31–50.
47. Evans, D.R., Myles, T., Hofsteenge, J., and Hemmings, B.A. (1999). Functional expression of human PP2Ac in yeast permits the identification of novel C-terminal and dominant-negative mutant forms. J. Biol. Chem. *274*, 24038–24046.
48. Migueleti, D.L., Smetana, J.H., Nunes, H.F., Kobarg, J., and Zanchin, N.I. (2012). Identification and characterization of an alternatively spliced isoform of the human protein phosphatase 2Aα catalytic subunit. J. Biol. Chem. *287*, 4853–4862.
49. Tang, S., Liu, Y., Wang, X., Liang, Z., Cai, H., Mo, L., Xiao, D., Guo, S., Ouyang, Y., Sun, B., et al. (2017). Characterization of overexpression of the alternatively spliced isoform of the protein phosphatase 2A catalytic subunit in cells. Biochem. Biophys. Res. Commun. *494*, 491–498.

The American Journal of Human Genetics, Volume *104*

Supplemental Data

De Novo Mutations Affecting the Catalytic Cα Subunit of PP2A, *PPP2CA*, Cause Syndromic Intellectual Disability Resembling Other PP2A-Related Neurodevelopmental Disorders

Sara Reynhout, Sandra Jansen, Dorien Haesen, Siska van Belle, Sonja A. de Munnik, Ernie M.H.F. Bongers, Jolanda H. Schieving, Carlo Marcelis, Jeanne Amiel, Marlène Rio, Heather Mclaughlin, Roger Ladda, Susan Sell, Marjolein Kriek, Cacha M.P.C.D. Peeters-Scholte, Paulien A. Terhal, Koen L. van Gassen, Nienke Verbeek, Sonja Henry, Jessica Scott Schwoerer, Saleem Malik, Nicole Revencu, Carlos R. Ferreira, Ellen Macnamara, Hilde M.H. Braakman, Elise Brimble, Maura R.Z. Ruznikov, Matias Wagner, Philip Harrer, Dagmar Wieczorek, Alma Kuechler, Barak Tziperman, Ortal Barel, Bert B.A. de Vries, Christopher T. Gordon, Veerle Janssens, and Lisenka E.L.M. Vissers

Supplemental data

Supplemental Case Reports of individuals with a *PPP2CA* mutation or partial deletion.

Individual 1

This 6-year-old boy was born at term after an uncomplicated pregnancy by caesarean section with Apgar scores of 9 and 10 after 1 and 5 minutes, respectively, and a birth weight of 3715 gram. He had laryngomalacia. His motor milestones were delayed: he could stand with support at the age of 12 months and could walk independently at the age of 20 months. At the age of 3 years he spoke several words. He attended special education and he is easily distracted and energetic. From 11 to 18 months he had atypical convulsions during fever. He had feeding difficulties.

Family history was unremarkable; he had 3 older, healthy, siblings.

Physical examination at the age of 6 years showed a height of 131 cm (+2 SD), weight of 26 kg (-0.2 SD) and head circumference of 56 cm (+2.5 SD). Target height was 175 cm (-1.2 SD). He had a broad forehead and frontal bossing, slight hypertelorism, prominent eyes, full nasal tip, low hanging columella, square shape of both ears, and short philtrum. Hands showed single palmar crease on the left side, long fingers and toes, and sandal gap on both sides. He had four small café-au-lait spots (< 0.5 cm). Brain MRI showed ventriculomegaly and enlargement of the subarchnoid space around the cerebrum without signs of increased cranial pressure. EEG, array-CGH and DNA analysis of *NSD1* (Sotos syndrome) and *PTEN* (PHTS) were normal. Whole exome sequencing revealed a *de novo* mutation in *PPP2CA* (c.572A>G; p.(His191Arg)).

Individual 2

This 7-year-old girl was born at term after an uncomplicated pregnancy and delivery and a birth weight of 3520 gram. After a few days she showed hypertonia and at the age of 4 months delayed development was noticed. At the age of 5.5 years she could make contact, sounds and was able to walk with foot casts and support.

From the age of 6 months she developed tonic-clonic convulsions, which changed into absences up to 50 times a day at the age of 5.5 years. She was diagnosed with epileptic encephalopathy and was treated with several medications including sodium valproate, levetiracetam, pyridoxine, clonazepam, rectal diazepam, alimemazine, multivitamins and had a ketogenic diet. She had severe sleeping problems and behavioural problems consisting of stereotypic behavior and automutilation. She had helmet therapy

because of plagiocephaly and was treated for malposition of the feet. She had feeding problems. She had normal vision, but hearing could not be tested.

Family history was unremarkable; she had one healthy brother.

Physical examination at the age of 6.5 years showed a height of 137 cm (+2.5 SD) and a weight of 30.2 kg (0 SD) and head circumference at the age of 1 year and 8 months was 48.3 cm (+0.5 SD). Physical examination at the age of 1 year and 8 months showed an open fontanel, plagiocephaly, some frontal bossing, broad nasal bridge, short philtrum, prominent upper lip, a sacral dimple, fetal finger pads and a single palmar crease on the left side. Skin showed no abnormalities. She had axial hypotonia and hypertonia of the legs with Babinski sign on both sides. Brain MRI showed central and peripheral ventriculomegaly, gracile corpus callosum and delayed myelination. MRS was normal.

Metabolic screening was normal and muscle biopsy showed no mitochondrial disease. DNA analysis of mtDNA, *UBE3A, MECP2, FOXG1, CDKL5* and analysis of methylation of the Angelman syndrome region and SNP-array were normal.

Whole exome sequencing revealed a *de novo* mutation in *PPP2CA* (c.882dup; p.(Arg295*)) and de novo variants of unknown significance in *ZNF687*; Chr1(GRCh37):g.151262240G>C; NM_020832.1:c.2721G>C (p.(Glu907Asp)), *MUC2*; Chr11(NCBI36):g.1088745T>C; NM_002457.2:c.7103T>C (p.(Leu2368Pro)), *FOXC2*; Chr16(GRCh37):g.86600973A>G; NM_005251.2:c.32A>G (p.(Asn11Ser)), *ARHGAP35*; Chr19(GRCh37):g.47423816A>G;NM_004491.4:c.1884A>G (p.Ile628Met)).

Individual 3

This 13-year-old boy was born at term after an uncomplicated pregnancy and delivery with a normal birth weight.

He had delayed development, could walk from the age of 2 years and started talking at the age of 4 years. His VIQ was 80 and PIQ 59, and he attended special education. He was diagnosed with PDD-NOS. His muscle tone was decreased. He had his first convulsion at the age of 10 years. He had focal epilepsy and convulsions mostly occurred at night. Electroencephalography demonstrated a left-temporo-occipital seizure focus, with an increase in focal epileptiform activity during sleep, fitting focal Electrical Status Epilepticus during Sleep (ESES). He was (previously) treated with levetiracetam, clobazam, methylprednisolone and lamotrigine.

He had feeding difficulties due to problems with chewing and (preparing the food for) swallowing, an open mouth posture, lack of facial expression, and articulation problems due to oral facial muscle

weakness. He was treated with vitamin B12 because of a vitamin B12 deficiency. He had no sleeping difficulties and normal vision and hearing.
His mother had one miscarriage and his sister died perinatally due to a coagulation defect of the mother. His father had two other children who were healthy.
Physical examination at the age of 11 years and 10 months showed a height of 164 cm (+1.3 SD), weight of 43.4 kg (-1.1 SD) and head circumference of 51.5 cm (-1.5 SD). He had periorbital fullness, restricted to the upper eyelids, long eyelashes and a full nasal tip. MRI of the brain, metabolic screening, array and DNA analysis of *PTEN* and *SCL2A1* showed no abnormalities.
Whole exome sequencing revealed a *de novo* mutation in *PPP2CA* (c.438del; p.(Phe146Leufs*29)).

Individual 4

This boy was the third child of healthy, non-consanguineous parents Family history was unremarkable. Pregnancy was complicated by diet-treated gestational diabetes mellitus. He was born full-term after normal delivery with Apgar scores of 9 and 10 after 1 and 2 minutes, respectively, and growth parameters in the normal range (birth weight 3450 gram, birth length 50 cm, OFC 36 cm). At birth he was noted to have bilateral adducted thumbs, unilateral camptodactyly of the third finger and umbilical hernia.
Development has been delayed. He could walk alone at the age of 19 months and had no spoken words at the age of 3.5 years. Physical examination at the age of 3 years and 10 months showed a height of 106 cm (+1.7 SD), weight of 16.7 kg (+0.7 SD) and head circumference of 46 cm (-3.9 SD). He had trigonocephaly, double hair whorl, short palpebral fissures, ptosis, low set and anteverted ears, high palate and retrognathia. Extremities showed a poorly developed flexure fold on the third finger of the right hand, an incomplete single transverse palmar crease and (reducible) adducted thumbs.
X-ray revealed ovoid appearance of vertebrae, coxa valga, slender distal phalanges and elevated right diaphragm. Abdominal ultrasound was normal. Cranial CT-scan ruled out craniosynostosis.
Brain MRI at the age of 2 years and 2 months showed posterior hypoplasia of corpus callosum, unmyelinated left temporal lobe and non-specific periventricular white matter hyperintensities.
Array-CGH and metabolic screening showed no abnormalities.
Whole exome sequencing revealed a *de novo* mutation in *PPP2CA* (c.922_924dup; p.(Phe308dup)).

Individual 5

This 19-year-old woman was born after a pregnancy complicated by oligohydramnios and delivery with a birth weight of 3742 gram. The baby suffered meconium aspiration but required no NICU stay. Development was delayed, and she had hypotonia. She could walk at the age of approximately 14 months, she spoke her first words prior to 2 years and had a language delay. She briefly stopped talking at the age of four years. She had a mild to moderate intellectual disability, and autism and ADHD. She had generalized tonic-clonic seizures and was diagnosed with Jeavons syndrome. She had constipation, a heart murmur, urinary urgency and recurrent ear and urinary tract infections.

Medical history showed wrist and foot fractures after minimal trauma. She had knee pain which limited daily activities and recently developed a burning pain from neck down through her left leg. She has had four periods of sudden vision loss in her left eye with blurry vision and pain. ERG was abnormal and additional studies are planned to further characterize an abnormal signal between her left and right eye. She had pigmented nevi and brownish waxy macules on the medial aspect left breast which might be caused by seborrhoeic keratosis.

Family history was unremarkable.

Physical examination at the age of 19 years showed a height of 162.8 cm (-0.2 SD), weight of 76.9 kg (>+2.5 SD) and BMI of 29. She did not have facial dysmorphisms but had crowded teeth. Extremities were unremarkable.

MRI at the age of 18 showed a T2 hyperintense focus within the left frontal lobe, likely a neural glial cyst. Array-CGH, DNA-analysis for Fragile X syndrome and lysosomal enzymes showed no abnormalities. Whole exome sequencing revealed a *de novo* mutation in *PPP2CA* (c.640 C>T; p.(Arg214*) and a mutation in *VWF* (NM_000552.3:c.2561G>A (p.Arg854Gln)) (Von Willebrand disorder).

Individual 6

This 2-year 4-month-old girl was born after a pregnancy complicated by a single umbilical artery on prenatal ultrasound. She was born at a gestational age of 39 weeks and 6 days with a normal birth weight. She received physiotherapy from the age of 6 weeks because of plagiocephaly. She refused breast feeding and after two weeks bottle feeding was started.

She was able to roll over from the age of 6 months and started to walk from the age of 2 years and 2 months. At the age of 2 years and 4 months she was babbling, did not use words, but did understand more than she could explain in words. At the age of 17 months, her development corresponded to that of a child of 13 months. BSID-II results showed a score of 61.

She had a fever-related tonic clonic insult twice. She had megalocornea, moderate excavated papillae and mild hypermetropia on both sides (+2).
She had a healthy older brother and a maternal aunt had attended special education.
Physical examination at the age of 1 year and 5 months showed a height of 80 cm (0 SD) and head circumference of 46.7 cm (-0.2 SD). She had plagiocephaly, prominent eyes, epicanthal folds, diastasis recti and mild shortened fifth digits.
Brain MRI showed a mildly underdeveloped pons and mesencephalon, mildly dilated lateral and third ventricles.
Metabolic screening and array-CGH showed no abnormalities.
Whole exome sequencing revealed a *de novo* mutation in *PPP2CA* (c.572A>G; p.(His191Arg)).

Individual 7

This 23-year-old female was born after an uncomplicated pregnancy and had a birth weight of ~2500 gram.
She could walk around the age of 12 months, had good fine motor skills, and possibly some mild hypotonia. Her language development was delayed: she spoke her first words at the age of two years, first sentences at age of four years and had speech therapy. At the age of seven years she had an IQ of ~130. At the age of 10 years ASD was diagnosed and her IQ was ~115. At the age of 16 years WISC-III showed a VIQ of 115 and a PIQ of 92. At the age of 17 years she had her first psychotic episode after which she had progressive cognitive dysfunction, with worsening of executive functions, and progressive behavioral problems defined by aggressive outbursts and episodes of confusion. At the age of 23 years she had a total IQ of ~100.
She had frequent airway infections as a young child.
Family history was unremarkable.
Physical examination at the age of 22 years showed a height of 175 cm (+0.7 SD) and head circumference of 60 cm (+2.8 SD). She had deep set eyes, small palpebral fissures, broad nasal tip, broad forehead and freckling around the mouth. Extremities showed no abnormalities.
Brain MRI, EEGs and metabolic screening were normal.
Array-CGH showed a paternally inherited duplication of ~223 kb at 4p15.2 and a maternally inherited duplication of ~1,68 Mb at Xp22.31.
Whole exome sequencing revealed a *de novo* mutation in *PPP2CA* (c. 668A>T; p.(Asp223Val)).

Individual 8

This 3-year-old girl was born after an uncomplicated pregnancy and delivery with Apgar scores of 9 and 10 after 1 and 2 minutes, respectively, and a birth weight of 3500 gram. Postnatally a clavicle fracture was diagnosed with torticollis to the right side. She had a muscular ventricular septal defect, which closed spontaneously.

Motor development was delayed because of hypotonia and hypermobility. Walking was achieved at the age of 35 months. Since she did not develop vocal language until the age of two, speech therapy was initiated. At the age of three years she could speak three-word sentences.

She had strabismus.

Family history was unremarkable.

Physical examination at the age of 2 years and 1 month showed a height of 83.5 cm (-1.3 SD), weight of 10.9 kg (-0.6 SD) and head circumference of 47 cm (-0.8 SD). She had plagiocephaly, megalocorneae (corneal diameter 13 mm), arched eyebrows, asymmetry of the nostrils, bifid nasal tip and hyperlaxity of the joints. Neurological examination revealed hypotonia with low symmetrical reflexes and a broad-based gait with hyperlordosis.

MRI at the age of 22 months showed a remarkably reduced amount of white matter, both supratentorial and infratentorial, some global atrophy of the brain (predominantly in the pontine and callosal area) and bilateral plexus choroideus cysts.

SNP array showed no abnormalities. Whole exome sequencing revealed a *de novo* mutation in *PPP2CA* (c. 373C>T; p.(Gln125*)). She also had a *de novo* variant of unknown clinical significance in *NIPBL* (NM_133433.3:c.3007_3009del; p.(Val1003del)), but was clinically not diagnosed with Cornelia de Lange syndrome.

Individual 9

This 21-month-old boy was born after a pregnancy complicated by preeclampsia and delivery by C-section with Apgar scores of 5 and 6 after 1 and 5 minutes, respectively, and a birth weight of 3324 gram.

Development was significantly delayed. He was not able to walk independently, was nonverbal and was not using signs.

He had hypotonia and cortical visual impairment due to an optic nerve anomaly. He had dysphagia for which he had tube feedings, and he had mild bilateral sensorineural hearing loss.

Family history was unremarkable.

Physical examination at the age of 1 year and 6 months showed a height of 84 cm (0.43 SD), weight of 10.8 kg (-0.2 SD) and head circumference of 43.4 cm (-3 SD). He had a prominent metopic suture, bilateral epicanthal folds and mild micrognathia. Extremities showed bridged palmar crease, ulnar deviation of wrists and fingers bilaterally, and partially adducted thumbs, right greater than left.
MRI at the age of 8 months showed pontocerebellar hypoplasia and mild ventriculomegaly.
Array CGH, gene panel for cerebellar/pontocerebellar genes (*AMPD2, CASK, CDK5, CHMP1A, EXOSC3, OPHN1, RARS2, RELN, SEPSECS, TSEN2, TSEN34, TSEN54, TUBA1A, TUBA8, TUBB2B, TUBB3, VLDR, VRK1*) and metabolic screening were normal.
Whole exome sequencing revealed a *de novo* mutation in *PPP2CA* (c.380A>G; p.(Tyr127Cys)).

Individual 10

This 8-year-old girl was born at term after an uneventful pregnancy. The neonatal period was unremarkable.
She walked independently at the age of 15 months and spoke in full sentences after the age of 3 years. She had a developmental delay, learning difficulties and autism spectrum disorder. At the age of 8 years she had normal gross motor development, a delay in fine motor development and significant speech delay for which she had speech therapy.
She started having seizures when she was 3 years old. On average she had 1-3 seizures per week and she has never been seizure-free for more than a month. She has been treated with multiple anticonvulsants including lacosamide, levetiracetam, zonisamide, and valproic acid which caused increase in seizure frequency according to the mother. She also underwent a brief trial of cannabidiol (CBD) oil.
Physical examination at the age of 8.5 years showed a height of 119.4 cm (-2 SD), weight of 19.6 kg (-1.5 SD) and head circumference of 48 cm (-2.3 SD). She had no dysmorphic features. She had poor comprehension but can follow one-step commands. Cranial nerves were grossly intact. She had hypotonia, but strength was normal in all four extremities. She had normal symmetrical deep tendon reflexes and she had normal stance and gait. No abnormal movements were appreciated.
EEGs previously showed bicentral temporal interictal spike and wave activity and other times frequent generalized spike and slow-wave activity. MRI of the brain at the age of 7 years showed no malformation of cortical development. Nonspecific thinning of the corpus callosum and apparent, nonspecific, mild volume loss of the cerebellum were noted.
Whole exome sequencing revealed a *de novo* mutation in *PPP2CA* (c.794A>G; p.(Tyr265Cys)).

Individual 11

This 2-year 4-month-old boy was born after a pregnancy characterized by small placental abruption. At 5 months intra-uterine growth retardation was noted. He was born at 35.5 weeks by vaginal delivery with a weight of 1740 gram (-2.6 SD), length of 40.5 cm (-3.1 SD) and OFC of 30.5 cm (-1.5 SD). The Apgar score was 8/9/9. The placental abruption was considered too small to explain the growth retardation. His evolution was characterized by feeding difficulties, gastro-esophageal reflux, constipation and recurrent respiratory infections. He had umbilical and bilateral inguinal hernia.

He had on motor physiotherapy from birth until the age of 28 months. He acquired a stable sitting position at the age of 12 months, walked independently at the age of 18 months and spoke his first words at the age of 16 months. He had some pronunciation difficulties. Amelioration was noted once myringotomy tubes were placed. His vocabulary is rich and at the age of 28 months, he was able to make sentences. His comprehension was always considered very good.

Family history was unremarkable.

Physical examination at the age of 2 years and 4 months showed a height of 80 cm (-3 SD), weight of 9.7 kg (-3 SD) and head circumference of 46.5 cm (-2 SD). He had frontal bossing, upslanting palpebral fissures, full cheeks, thin upper lip and everted/prominent lower lip, retrognathia, and square configuration of the ear lobule (right>left). Extremities showed bilateral 5^{th} fingers clinodactyly.

Imaging of the brain was not performed. Metabolic screening showed no abnormalities. There was no methylation abnormality at the 11p15.5 locus and no maternal uniparental disomy for chromosome 7. SNP-array showed a *de novo* 120.36 kb deletion including the 5' region of *PPP2CA* and the 3' region of *CDKL3* (chr5:133,546,961-133,667,321) and a maternally inherited 353.74 kb deletion at chr18:63,620,373-63,974,115 in which no genes were located.

Individual 12

This 11-year-old boy, the first child to non-consanguineous parents, was born at 38 weeks' gestation after an uneventful pregnancy with a birth weight of 4140 gram. At birth he had poor suck and could not breastfeed well, so he was switched to special feeding at 2 weeks of age. Parents were concerned because of lack of milestone acquisition at 6 months of age, as by then he was still unable to hold his head or sit with support. By this point in time, he also didn't track well, and kept his hands in a clenched position.

At the age of 3 years and 10 months he was unable to sit, remained nonverbal and had minimal eye contact. Vineland Adaptive Behavior Scales (second edition) were administered at that point and

revealed a communication standard score of 42 (age equivalent approximately 1-2 months), daily living standard score of 48 (age equivalent approximately 0-2 months), socialization standard score of 53 (age equivalent approximately 0-4 months), and motor skills standard score of 28 (age equivalent approximately 1 month).

At 8 months of age he developed abnormal movements and subsequently experienced an afebrile tonic clonic seizure. He went on to have several seizure types, including staring spells, head drops, and tonic clonic seizures. At 10 months, an EEG was performed and revealed hypsarrhythmia (West syndrome). Despite treatment with multiple antiepileptic drugs (lamotrigine, levetiracetam, topiramate), he continued to have 1-2 seizures per day.

He developed chronic constipation starting at 1 year of age. He had an ASD (atrial septal defect) and low bone mineral density (Z-score -2.7 at spine L1-L4).

Physical examination at the age of 3 years and 10 months showed a height of 94.5 cm (-1.6 SD), weight of 12.5 kg (-2.1 SD) and head circumference of 48.5 cm (-1.1 SD). He had no dysmorphic features. His neurologic exam revealed truncal hypotonia, and adventitial movements consistent with choreiform activity in all four limbs.

Brain MRI showed no structural abnormalities, but slight accentuation of the contrast between gray matter and white matter. Brain MRS showed low NAA (N-acetylaspartate) and elevated choline at several locations studied. Extensive metabolic workup was unremarkable. Karyogram, chromosome microarray, DNA analysis for Fragile X syndrome*, MECP2, ARX, CLN1, CLN2, COX10, SCO2, SURF1, SCO1, POLG1* and mitochondrial DNA were normal.

Whole exome sequencing revealed a *de novo* mutation in *PPP2CA* (c.391G>C; p.(Asp131His)).

Individual 13

This 12-month-old boy was born at 37 weeks via Caesarean section for oligohydramnios and breech positioning. Apgar scores were 7 and 8 at 1 and 5 minutes, respectively. Prenatal ultrasound showed microcephaly. After birth, he was transferred to the NICU for respiratory distress, a heart murmur, and for small size. Measurements for birth weight, length, and head circumference were all greater than 2 standard deviations below the mean. He required CPAP for one day.

At 5 months of age, he had several episodes of sudden bilateral upper and lower extremity extension, with loss of tone and post-ictal perioral cyanosis and was started on levetiracetam. He continued to have breakthrough seizures on maximal dosing and was transitioned to oxcarbazepine, which has provided adequate seizure control.

He had global developmental delay. At 11 months of age, the Capute scales documented significant delays in language and cognition, with a CLAMS Developmental Quotient of 73 and a CAT Developmental Quotient of 21. Gross motor age equivalency was determined to be approximately 5 months through the Bayley Motor Scale. He had a trileaflet aortic valve. He had a normal neuro-ophthalmology exam apart from intermittent exotropia.

Family history was unremarkable.

Physical examination at the age of 12 months showed a height of 71.5 cm (-1.9 SD), weight of 7.9 kg (-1.9 SD) and head circumference of 40.2 cm (-4.6 SD). He had bilateral single palmar crease and adducted thumbs and several hyperpigmented macules, some with irregular borders. He has global hypotonia and hyperreflexia in the lower extremities.

His EEGs have captured clinical events with electrographic correlate arising from the left central and posterior regions with some multifocal sharps and spikes. There has not been evidence to date of an epileptic encephalopathy.

Brain imaging at 5 months demonstrated microcephaly, enlarged subarachnoid spaces, and additional nonspecific findings of cerebral underdevelopment.

Chromosomal microarray identified a maternally inherited ~347 kb duplication of uncertain significance at chromosome 7q11.22. This duplication includes the terminal portion of one gene, *AUTS2*. Whole exome sequencing revealed a *de novo* mutation in *PPP2CA* (c.366G>A; p.(Gln122His)).

Individual 14

This 4-year-old girl was born at a gestational age of 39 weeks. She had hyperbilirubinemia on the fourth day of life requiring phototherapy until the eighth day of life. Primary microcephaly was noticed in the neonatal period. Tonic-clonic seizures and recurring vomiting started in the first year of life. Epilepsy was refractory to an initial therapy with topiramate and primidone as well as phenobarbital, but seizure frequency initially responded to a combination of levetiracetam and topiramate.

She had severe combined developmental delay and does not speak which could be partially explained by her being a refugee. She had no regression. She had severe truncal hypotonia.

Family history was unremarkable.

Physical examination at the age of 4 years showed a height of 99 cm (-0.8 SD), weight of 15 kg (-0.6 SD) and head circumference of 41 cm (< -2 SD). She presented with striking stereotypies. She had large, almond shaped eyes, small mouth, high palate, and an atypical single palmar crease on the left hand, pes planus and overlapping toes.

Continuous generalized deceleration was seen in EEG indicating diffuse brain dysfunction.
A suspicious craniocervical passage was reported in an MRI at the age of 6 months. An MRI at the age of 2 years showed slightly dilated external and internal subarachnoid spaces but no abnormalities of the craniocervical passage. Additionally, MRI showed diffuse but discrete atrophy, adequate myelination.
Whole exome sequencing revealed a *de novo* mutation in *PPP2CA* (c.263A>G; p.(Asp88Gly)).

Individual 15

This 3-year-old boy was born at term after an uneventful pregnancy and delivery with a birth weight of 3620 gram and Apgar scores of 10 and 10 at 1 and 5 minutes, respectively. In the first year of life, he cried frequently and was difficult to comfort and to handle. His psychomotor development was delayed; he was supported by physiotherapy and later by early support therapy. He started walking at the age of 18 months and spoke his first words at 18 months. At 2 years of age, his active vocabulary comprised 5 words, but he had a better speech comprehension. Upon clinical re-evaluation at age 3 years and 4 months, his development was delayed by 1-1.5 years. He showed behavioral anomalies with recurrent episodes of screaming and crying.
Family history was unremarkable.
Physical examination at the age of 3 years and 4 months showed a height of 99 cm (0 SD), weight of 17 kg (+1.2 SD) and head circumference of 48 cm (-2 SD). His craniofacial features were not dysmorphic; he had a small broad nasal tip with small alae nasi. He had a single palmar crease at his left hand and a sacral hemangioma.
EEG, cranial MRI scan, and audiometric testing were all normal.
Chromosome analysis by karyotyping was normal (46,XY), array analysis showed a paternally inherited 4q31.3 duplication of 398 kb in size, which was upon re-evaluation classified as benign CNV. Whole exome sequencing revealed a *de novo* mutation in *PPP2CA* (c.179G>T; p.(Gly60Val)).

Individual 16

This 7-year-old boy was born at term. At the age of 1 year he had his first generalized seizures and was successfully treated with valproate, but then suffered autistic regression and the treatment was changed to topiramate. After a few seizure free months, the topiramate was stopped. At the age of 6 years he started to have generalized seizures again and had a few status epilepticus events. He was treated with levetiracetam without success and could not tolerate lamotrigine. At the age of 7 years he was treated

with valproate, clobazam and topiramate. He had drug resistant epilepsy with generalized seizures on a daily basis, mostly upon awakening, and was about to start medical cannabis.

He was diagnosed with severe autistic spectrum disorder requiring permanent supervision and severe developmental delay with a Developmental Quotient lower than 50.

He had healthy parents. His brother had cerebral palsy due to perinatal stroke.

Physical examination at the age of 7 years showed a height of 113 cm (-2 SD), weight of 20 kg (-1.5 SD) and head circumference of 52.8 cm (0 SD).

Metabolic screening was normal. EEG at the age of 7 years showed general spike and wave activity corresponding with limb tremor and staring. Brain MRI at 1 year of age was normal, brain MRI at the age of 3 years showed mild dilatation of perivascular spaces and brain MRI at the age of 7 years showed more marked dilatation of perivascular spaces along the corona radiata bilateral.

Chromosomal microarray showed no abnormalities.

Whole exome sequencing revealed a *de novo* mutation in *PPP2CA* (c.667G>C; p.(Asp223His)).

Figure S1: Binding of mutant PP2A Cα subunits to B-type subunits

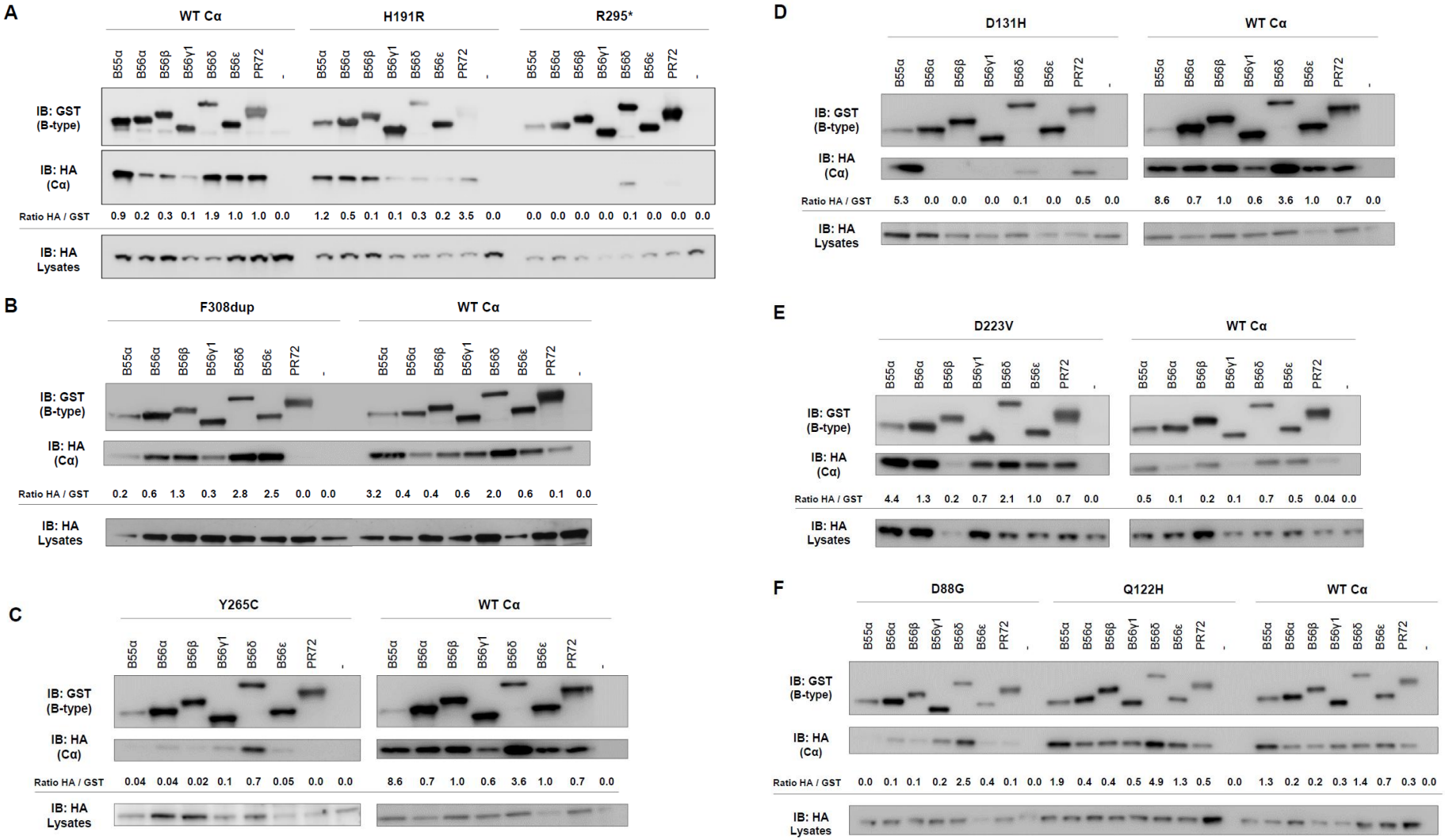

G

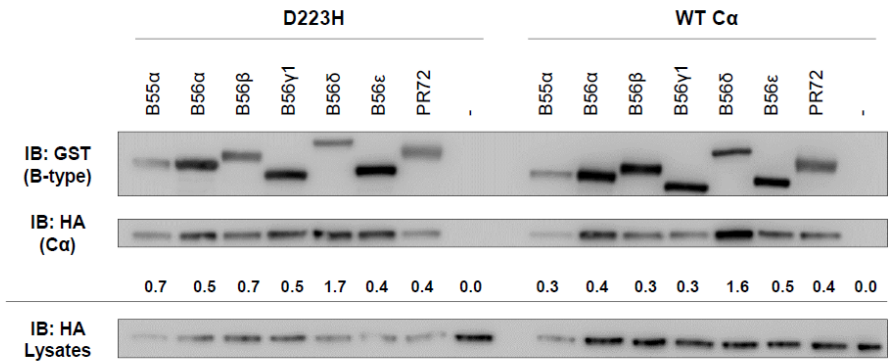

Legend Figure S1.

A-G. GST-tagged B-type subunits were co-expressed with HA-tagged WT or mutant Cα proteins (H191R, R295*, F308dup, Y265C, D131H, D223V, D88G, Q122H and D223H) in HEK293T cells. The presence of the PP2A C variants was subsequently assessed in GST pull downs by anti-HA immunoblotting. Each blot is a representative image of at least n=3.

Table S1. Oligonucleotides used for site-directed mutagenesis.

G60V Forward	5’-GTCTGTGGAGATGTGCATGTGCAATTTCATGATCTCATG-3’
G60V Reverse	5’-CATGAGATCATGAAATTGCACATGCACATCTCCACAGAC-3’
D88G Forward	5’-CTTGTTTATGGGAGATTATGTTGGCAGAGGATATTATTCAGTTGAAA-3’
D88G Reverse	5’-TTTCAACTGAATAATATCCTCTGCCAACATAATCTCCCATAAACAAG-3’
Q122H Forward	5’-GGAATCATGAGAGCAGACACATCACACAAGTTTATGGTT-3’
Q122H Reverse	5’-AACCATAAACTTGTGTGATGTGTCTGCTCTCATGATTCC-3’
Q125* Forward	5’-CATGAGAGCAGACAGATCACATAAGTTTATGGTTTCTATGATG-3’
Q125* Reverse	5’-CATCATAGAAACCATAAACTTATGTGATCTGTCTGCTCTCATG-3’
Y127C Forward	5’-GAGCAGACAGATCACACAAGTTTGTGGTTTCTATGATGAATG-3’
Y127C Reverse	5’-CATTCATCATAGAAACCACAAACTTGTGTGATCTGTCTGCTC-3’
D131H Forward	5’-CAGATCACACAAGTTTATGGTTTCTATCATGAATGTTTAAGAAAATATGGAAAT-3’
D131H Reverse	5’-ATTTCCATATTTTCTTAAACATTCATGATAGAAACCATAAACTTGTGTGATCTG-3’
F146fs Forward	5’-GTTTGGAAATATTTACAGATCTTTTTGAC-3’
F146fs Reverse	5’-GTCAAAAAGATCTGTAAATATTTCCAAAC-3’
H191R Forward	5’-GCCTACAAGAAGTTCCCCGTGAGGGTCCAATGTGTGACTTG-3’
H191R Reverse	5’-CAAGTCACACATTGGACCCTCACGGGGAACTTCTTGTAGGC-3’
R214* Forward	5’-GTTGGGGTATATCTCCTTGAGGAGCTGGTTACACC-3’
R214* Reverse	5’-GGTGTAACCAGCTCCTCAAGGAGATATACCCCAAC-3’
D223H Forward	5’-GCTGGTTACACCTTTGGGCAACATATTTCTGAGACATTTAATC-3’
D223H Reverse	5’-GATTAAATGTCTCAGAAATATGTTGCCCAAAGGTGTAACCAGC-3’
D223V Forward	5’-CTGGTTACACCTTTGGGCAAGTTATTTCTGAGACATTTAATCA-3’
D223V Reverse	5’-TGATTAAATGTCTCAGAAATAACTTGCCCAAAGGTGTAACCAG-3’
Y265C Forward	5’-GATTTTCAGTGCTCCAAACTGTTGTTATCGTTGTGGTAACC-3’
Y265C Reverse	5’-GGTTACCACAACGATAACAACAGTTTGGAGCACTGAAAATC-3’
R295* Forward	5’-GCAGTTTGACCCAGCACCTCGTTGAGGCGAGCCACATGTTACTC-3’
R295* Reverse	5’-GAGTAACATGTGGCTCGCCTCAACGAGGTGCTGGGTCAAACTGC-3’
F308dup Forward	5’-GATTACGCTTCTAGAATGGACGAGAAGGTGTTCACC-3’
F308dup Reverse	5’-ATCATGTCTGGATCCTTACAGAAAGAAGTAGTCTGGGGTACGACG-3’